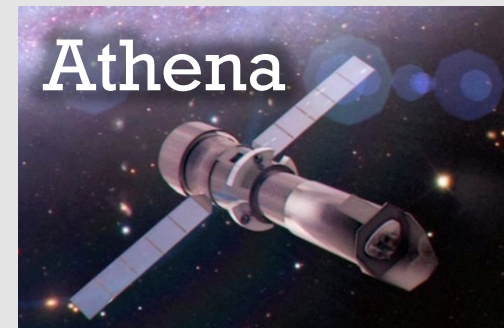
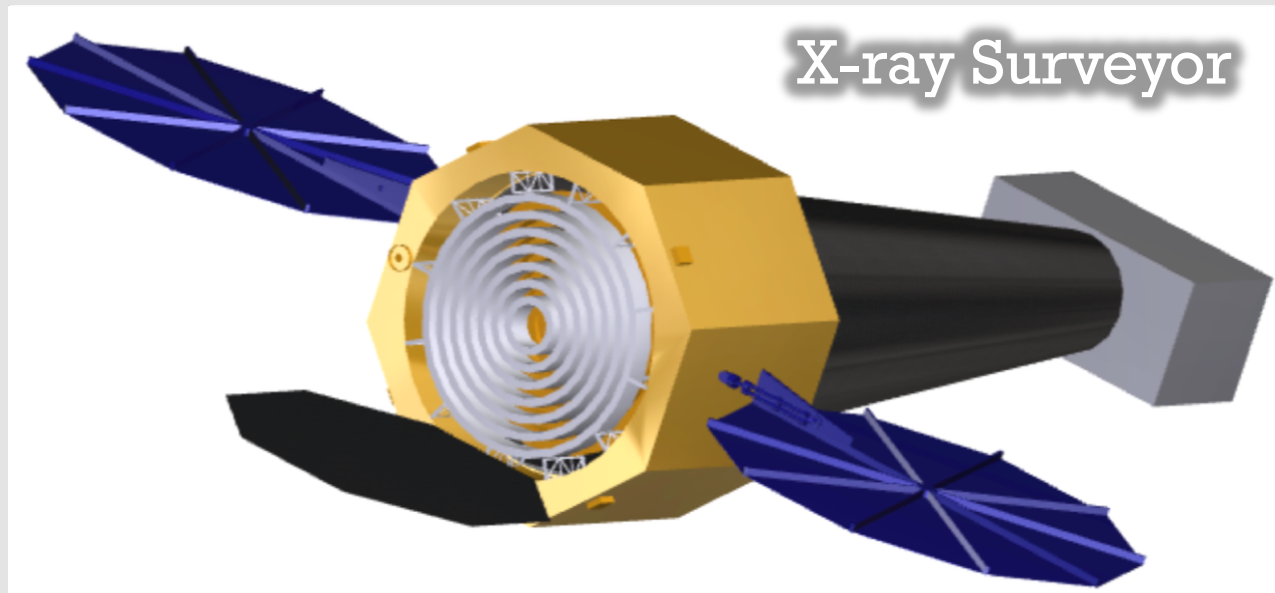


Observing the First Accretion Light with X-ray Surveyor

Niel Brandt (Penn State)



Working Group Members

James Aird

Niel Brandt

Nico Cappelluti

Francesca Civano

Andrea Comastri

Paolo Coppi

Anastasia Fialkov

Francesca Fornasini

Elena Gallo

Melanie Habouzit

Zoltan Haiman

Phil Kaaret

Joe Lazio

Bin Luo

Piero Madau

Takamitsu Miyaji

Dan Schwartz

Dan Stern

Benny Trakhtenbrot

Cristian Vignali

Fabio Vito

Marta Volonteri

The Most Compelling *X-ray Surveyor* Science Goals (“Killer Apps”) on First Accretion Light

Summary Title for Killer App:

Nature of First X-ray Sources

People Contributing Text to Describing this Killer App:

Anastasia Fialkov (CfA),

General Science Goal:

First population of X-ray sources has not been observed yet and several candidates have been discussed in literature including X-ray binaries (which are the leading candidates), mini-quasars, hot gas in galaxies, shocks, dark matter annihilation, etc. First X-ray sources had dramatic impact on the evolution of the Universe by heating up the intergalactic medium (IGM) and modifying spectrum and fluctuations of the 21-cm signal of neutral hydrogen before Reionization ($z > 6$). In particular, (1) because of cosmic heating the 21-cm signal of neutral hydrogen is predicted to transit from absorption regime to emission at redshift which depends on both the spectral energy distribution (SED) and efficiency of X-ray sources; (2) mean free path of X-ray photons at high redshifts is imprinted in the power spectrum of the 21-cm signal; and (3) depending on the nature of the first X-ray sources the 21-cm signal from the first half of Reionization ($z > 10$) can be heating-driven.

First X-ray sources can be directly resolved by X-ray Surveyor if they are bright enough, or contribute to the cosmological unresolved X-ray background. Putting together direct observations of first X-ray sources probed by X-ray Surveyor with future 21-cm measurements could help to constrain their nature. Moreover, it will allow to extract other astrophysical parameters from the 21-cm data with greater precision. It would be particularly useful to cross-correlate the large-scale fluctuations in the X-ray background with the 21-cm signal observed by the Square Kilometer Array (SKA) to establish the global effect of heating, the SED of these sources as well as properties of first star forming regions.

Specific Observational Goal:

1. Large-scale fluctuations of X-ray background: root mean square fluctuations of X-ray background at comoving 3 Mpc scale produced at $z = 9$ should be of $4 \times 10^{-15} \text{ erg/s/cm}^2/\text{keV per deg}^2$, and of 4×10^{-16} if produced at $z = 13$. If high-redshift fluctuations of X-ray background at comoving scales of $k < 1 \text{ Mpc}^{-1}$ will be measured, they can be cross-correlated with future 21-cm measurements by the SKA. Because the

Current Status and the Near Future

General Observational Status

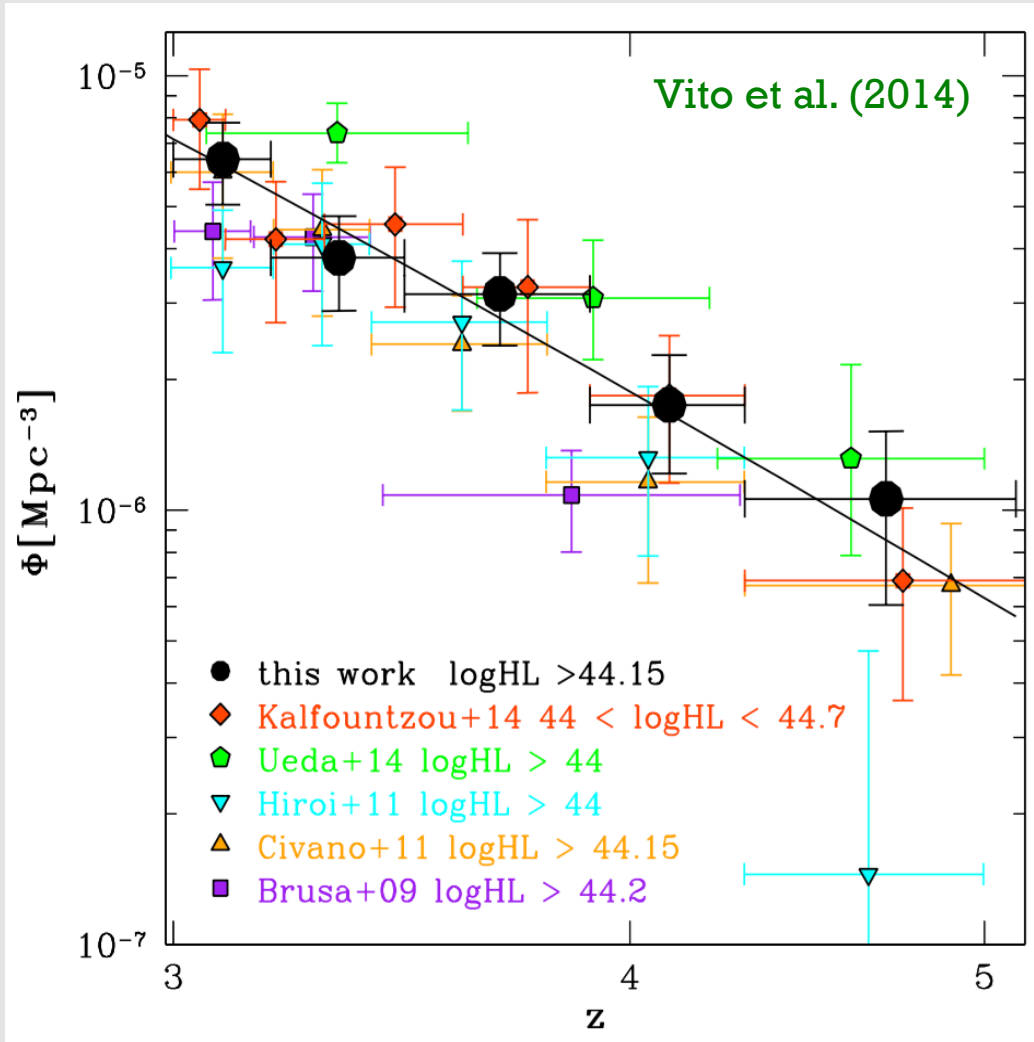
Over the past ~ 17 yr, the capabilities of Chandra and XMM-Newton have allowed a large expansion in the number of X-ray detected AGNs at $z = 4-7$.

X-ray follow-up of high-redshift AGNs first found in other multiwavelength surveys; e.g., SDSS, PSS, FIRST.

X-ray selected high-redshift AGNs in X-ray surveys.
Critical since X-rays penetrating and not diluted.

Now have about 155 X-ray detections at $z = 4-7$, allowing reliable basic X-ray population studies out to the reionization era.

Space Density Declines for High-Luminosity X-ray AGNs



In contrast to early suggestions from ROSAT, clearly see \sim exponential decline for luminous X-ray selected AGNs at $z > 3$.

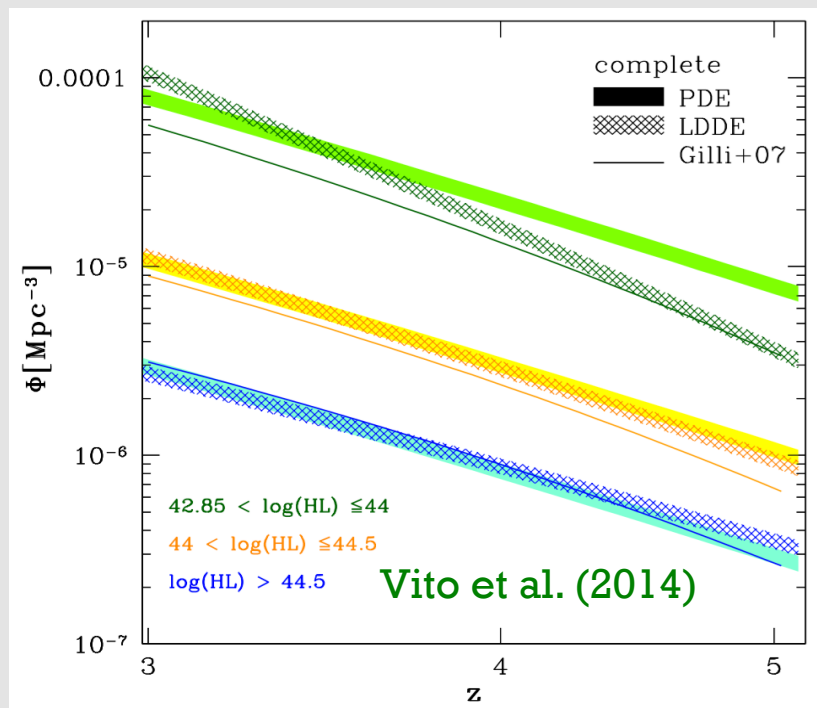
$$\Phi \propto (1+z)^p \text{ with } p = -6.0 \pm 0.8$$

Space-density comparisons with optically selected quasars indicate agreement to within factors ~ 2 -3.

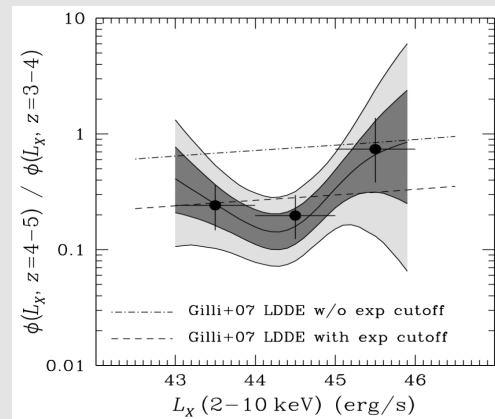
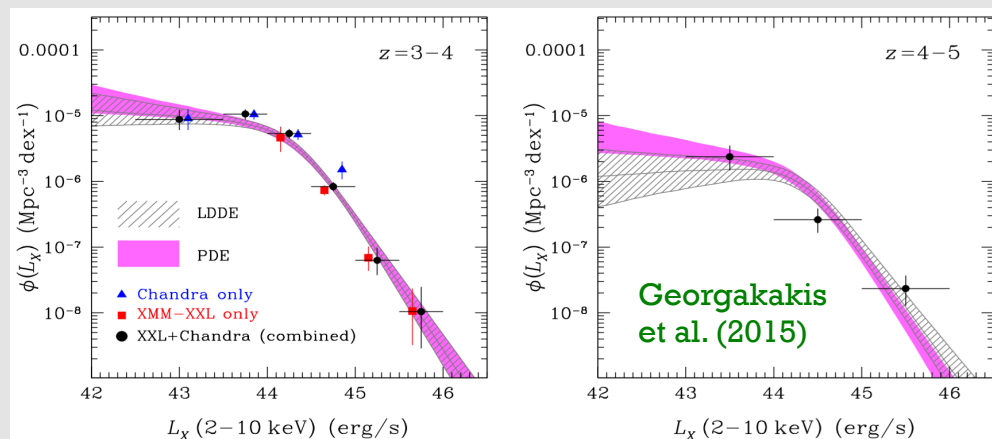
Space Density at $z \sim 3-5$ for Moderate-Luminosity X-ray AGNs

Remaining debate here – small samples, tough follow-up, results can depend on analysis details.

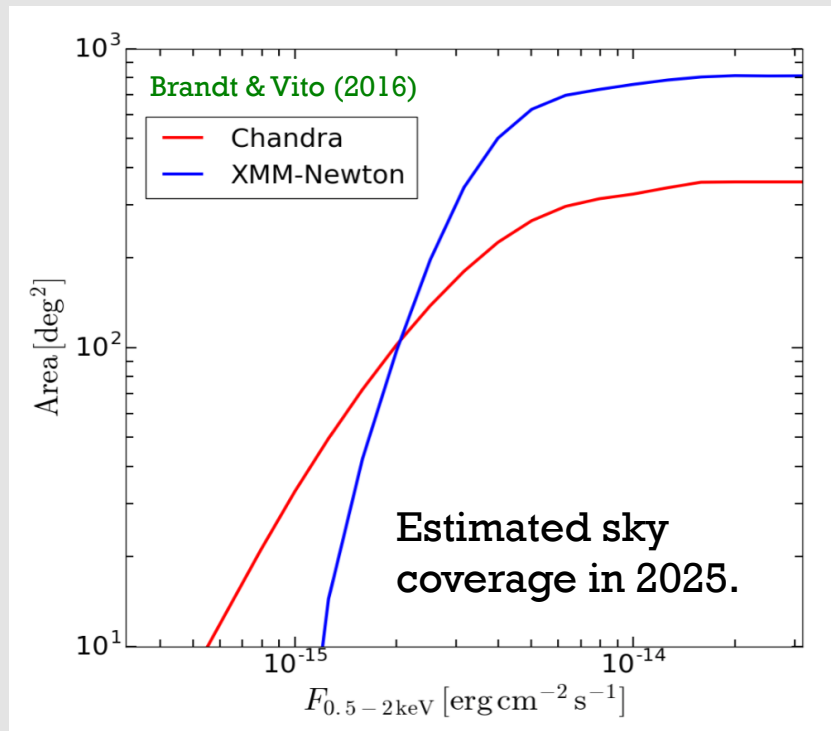
Similar Decline at Moderate Luminosities as at High Luminosities?



Drop by a Factor of ~ 5 from $z = 3-4$ to $z = 4-5$, but with Perhaps a Milder Drop at High Luminosities?

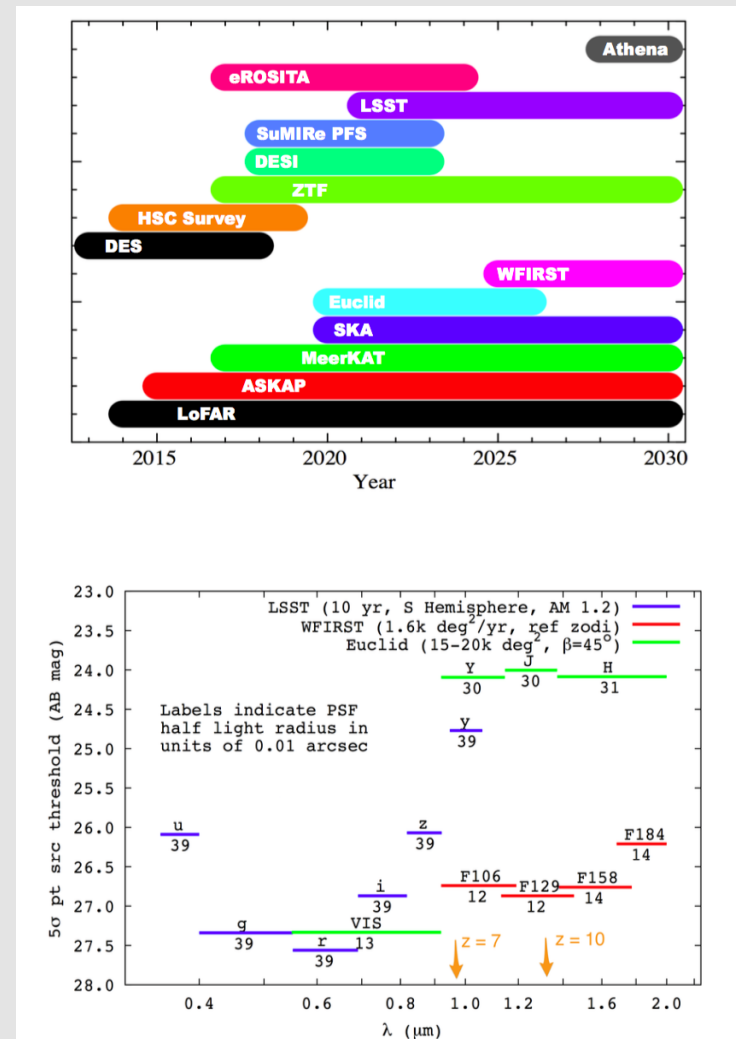


Status of High-Redshift X-ray AGN Surveys in a Decade



LSST/Euclid/WFIRST will make Chandra and XMM archives (and hopefully eROSITA) extremely powerful for finding obscured AGNs at $z = 4-8$.

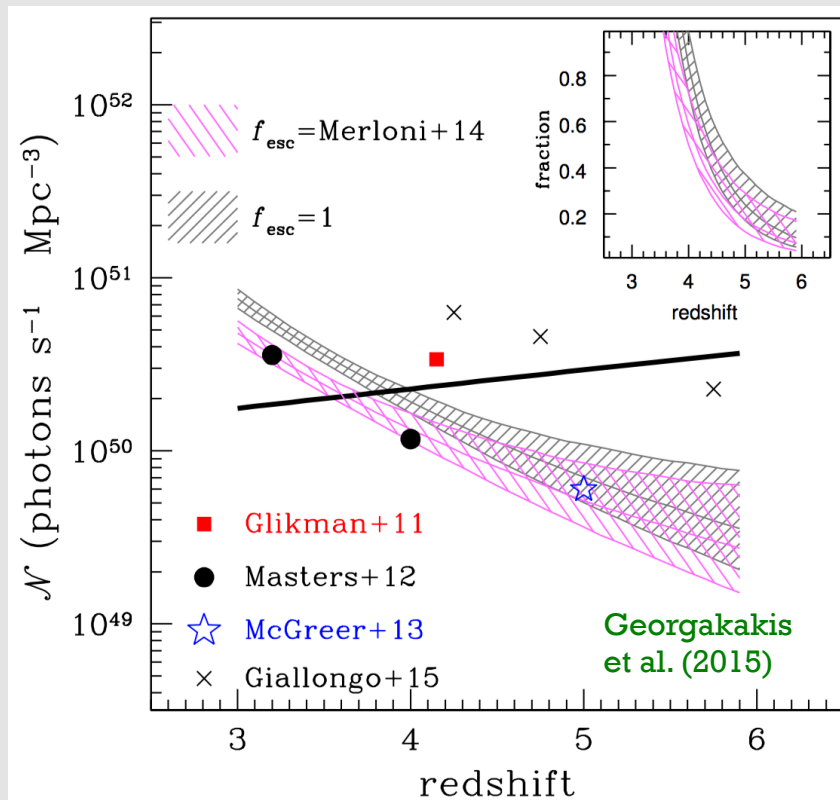
Plausibly expect 500-1100 AGNs at $z = 4-6$ and 10-100 at $z = 6-8$.



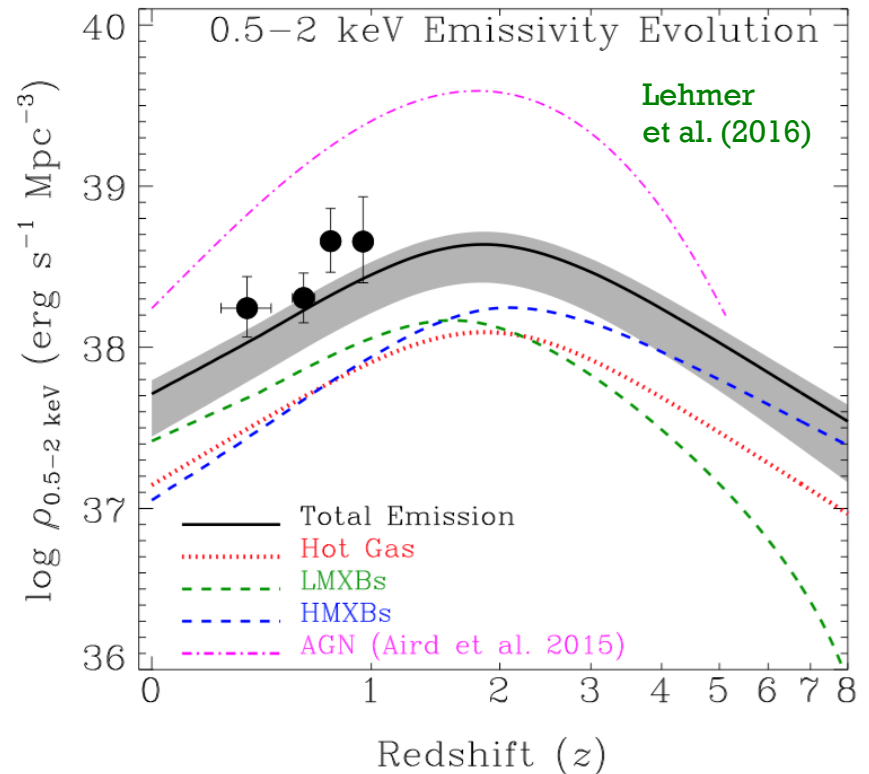
AGNs Probably Cannot Drive Reionization at $z \sim 6$

But AGNs and HMXBs likely have secondary IGM heating effects.

Hydrogen Ionizing Photon Rate Density from AGNs as Function of Redshift

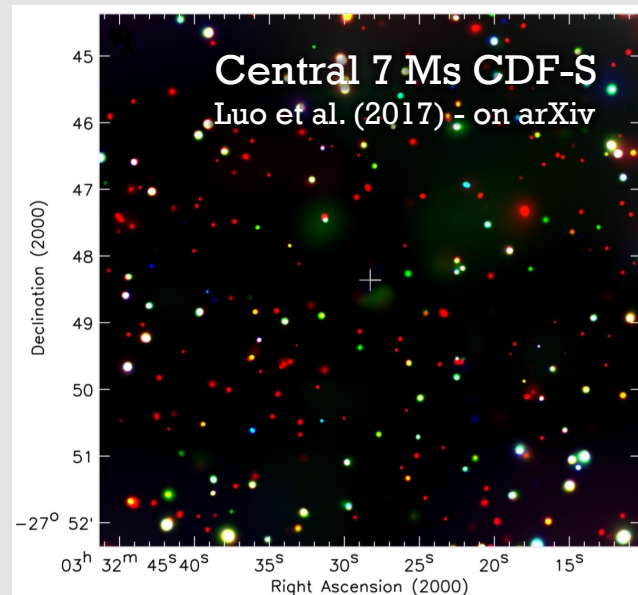
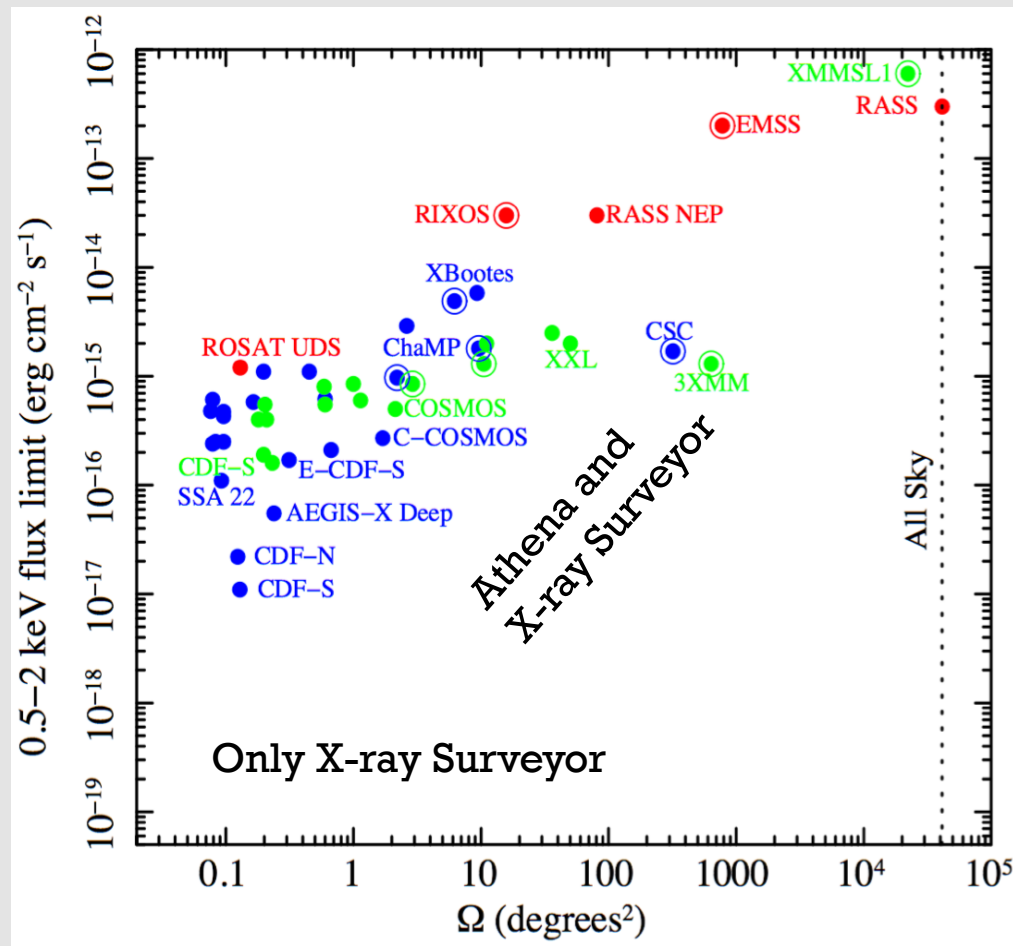


The Revenge of the X-ray Binaries at $z \sim 6-8$? (ρ_{Gal} May Drop Off More Slowly Than ρ_{AGN})



Seeds of First SMBHs with X-ray Surveyor

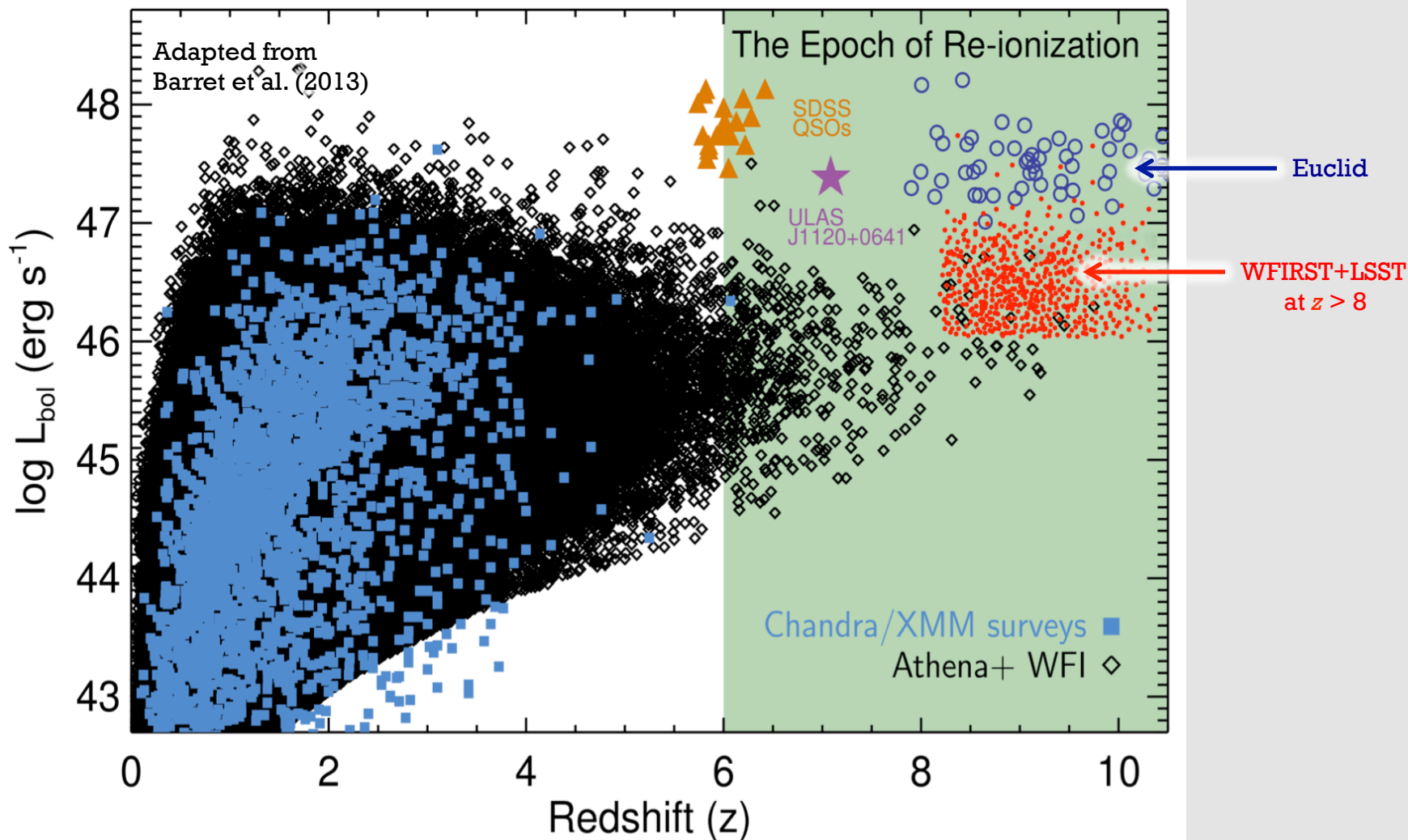
Seeds of SMBHs with X-ray Surveyor

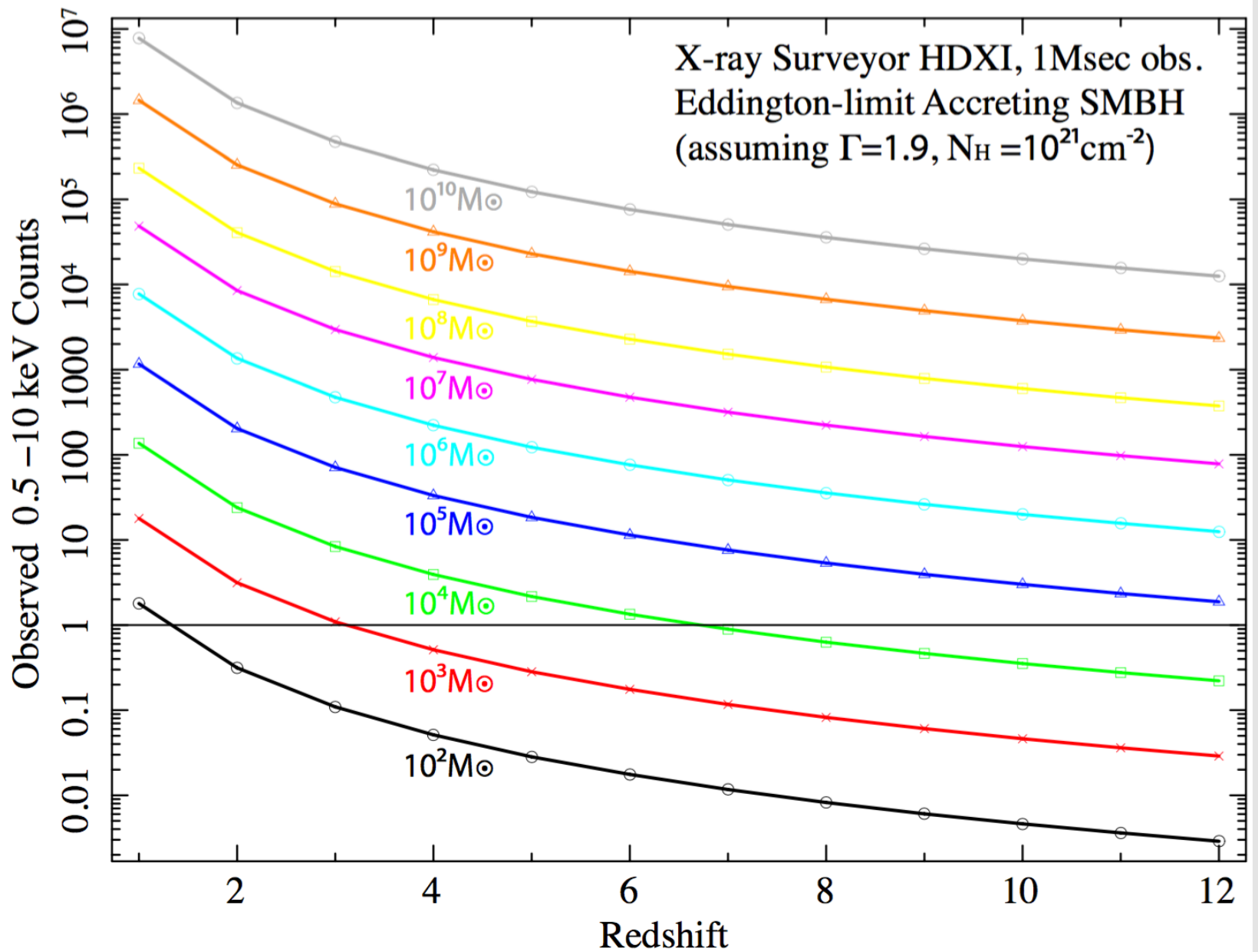


Need excellent X-ray surveyor imaging to push to X-ray fluxes far below Chandra (and get reliable counterparts).

At $z \sim 10$, can detect BH to $\sim 5 \times 10^4 M_{\odot}$, including obscured systems. Ideally would go a factor of several deeper still, so this is a challenging driver for X-ray Surveyor!

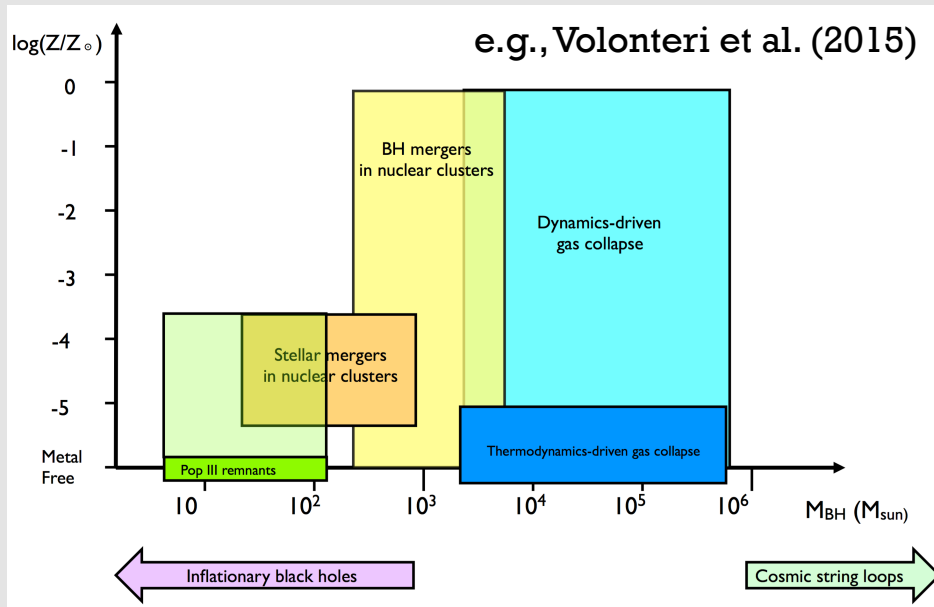
AGNs from 25 Ms Athena Survey versus Euclid and WFIRST+LSST





From Laura Brenneman

Seeds of SMBHs with X-ray Surveyor



Is super-Eddington growth of seeds possible?

Low-mass seeds with \sim uninterrupted rapid accretion?

Massive seeds from direct-collapse black holes?

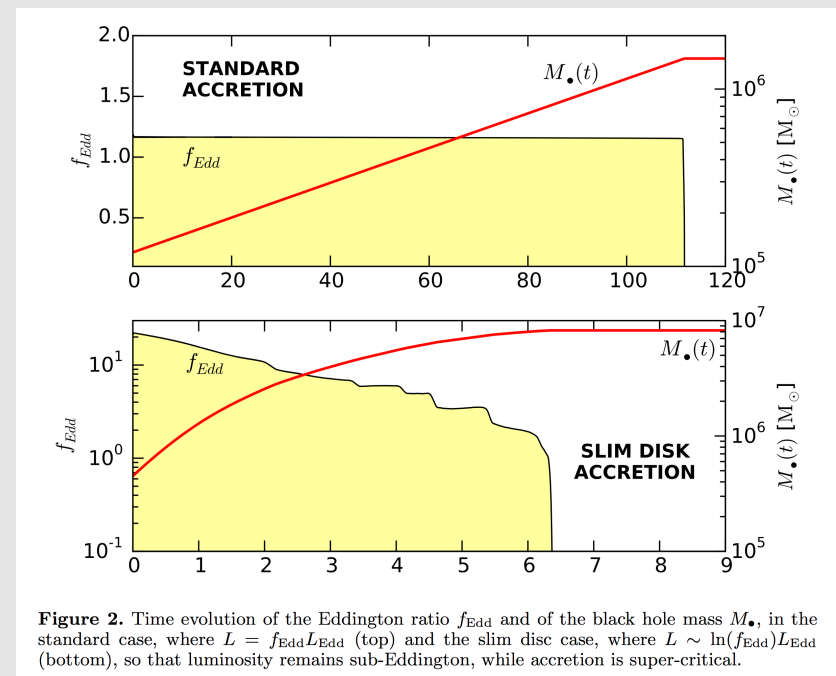


Figure 2. Time evolution of the Eddington ratio f_{Edd} and of the black hole mass M_{\bullet} , in the standard case, where $L = f_{\text{Edd}} L_{\text{Edd}}$ (top) and the slim disc case, where $L \sim \ln(f_{\text{Edd}}) L_{\text{Edd}}$ (bottom), so that luminosity remains sub-Eddington, while accretion is super-critical.

Constraining Seeds with the XLF

The behavior of the high-redshift X-ray luminosity function (XLF) at the very faint end will be key for insights into seed-growth models.

Growth from light seeds should lead to a large number of faint high-redshift AGN fueled by accretion onto low-mass BH.

For heavy seeds, AGNs can more easily reach luminosities close to L_* , producing a flatter faint end of XLF.

Our stacking-analysis constraints suggest a fairly flat end of the XLF.

Improved quantitative predictions of XLF behavior for different seed models will be most helpful. As well as other observables that can distinguish light vs. heavy seeds.

Example X-ray Surveyor Program

Need to reach 0.5-2 keV flux limits of at least 2×10^{-19} erg cm⁻² s⁻¹, and ideally want to reach a factor of several deeper still.

Sky-density estimates of seeds remain uncertain, but likely need to cover several deg² to such flux levels.

Probably best to obtain this sky coverage over several distinct fields to reduce cosmic variance effects while still probing any LSS.

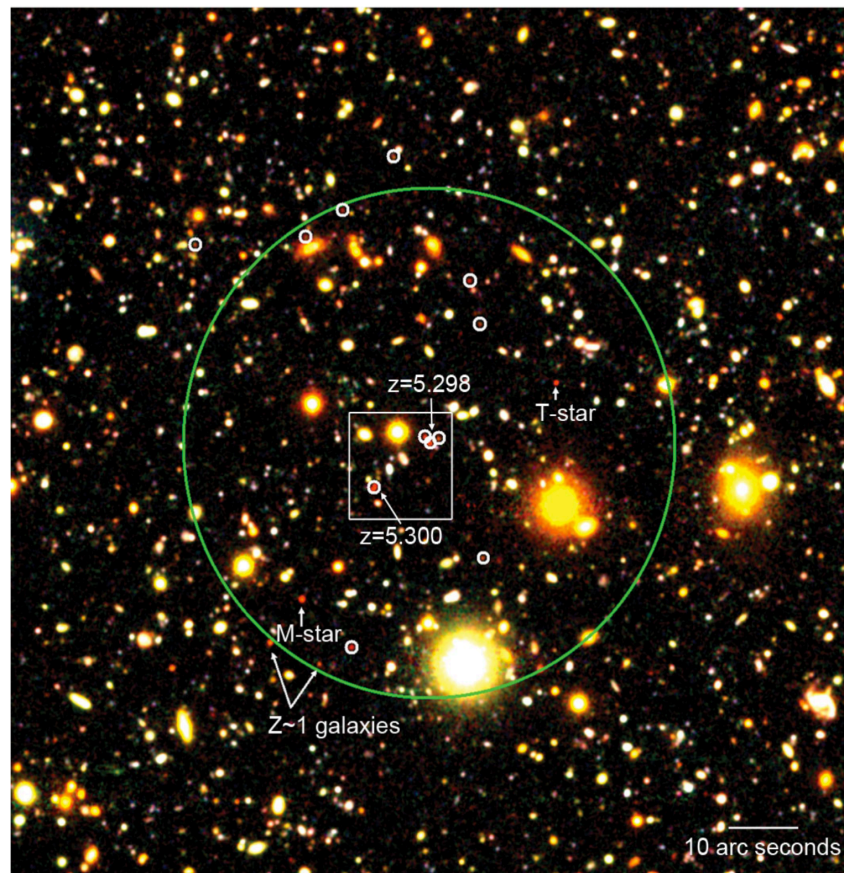
Will need to choose best fields around the time of launch, but likely candidates presently are, e.g., CDF-S, CDF-N, XMM-LSS, COSMOS.

Will be especially important to have ultradeep JWST, 21-cm, etc. data that can provide reliable counterparts.

X-ray source positions better than 0.5'' are needed for reliable source matching.

Environmental Dependence of the First SMBH Growth

$z = 5.3$ protocluster



Capak et al. (2011)

Currently, large-scale structures are found up to $z \sim 5-6$ in deep multiwavelength surveys - protoclusters and protogroups.

AGNs have been effective tracers for these.

Want to identify many more such structures in wide-field deep surveys with X-ray Surveyor, as well as push to higher redshifts.

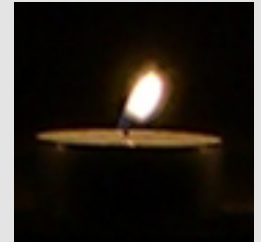
After detecting AGN tracers in X-ray band, identify with follow-up imaging and spectroscopic observations (e.g., JWST).

Enable statistical studies of the environmental dependence of the first SMBH growth.

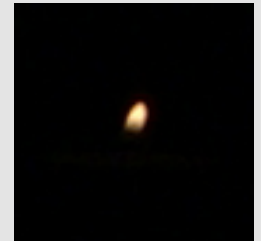
Stacking: A Romantic Example



3 / 100 second
exposure



1 / 1000 second
exposure



Courtesy of Bret Lehmer



Stacked image of 30 candles with 1 / 1000 sec exposure.

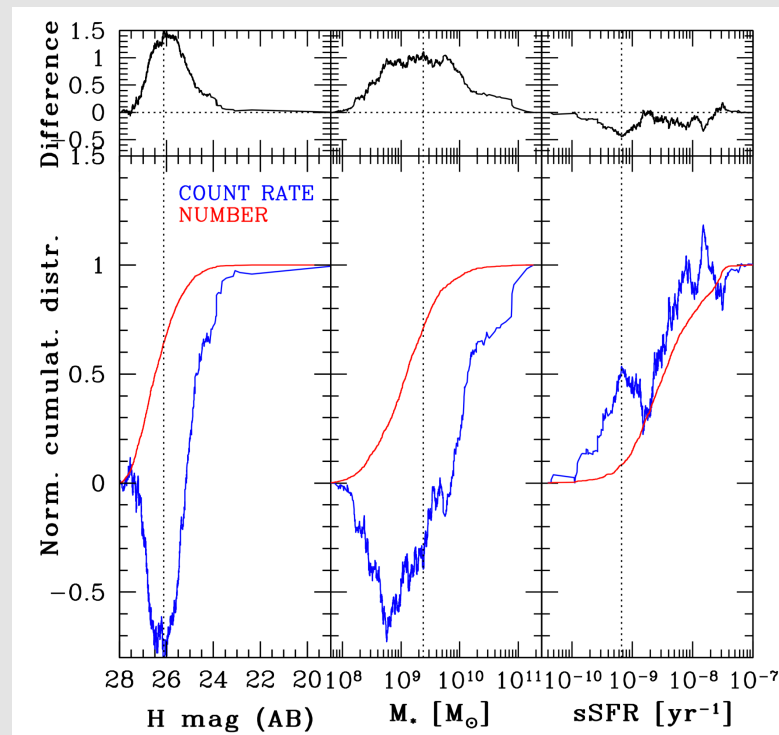
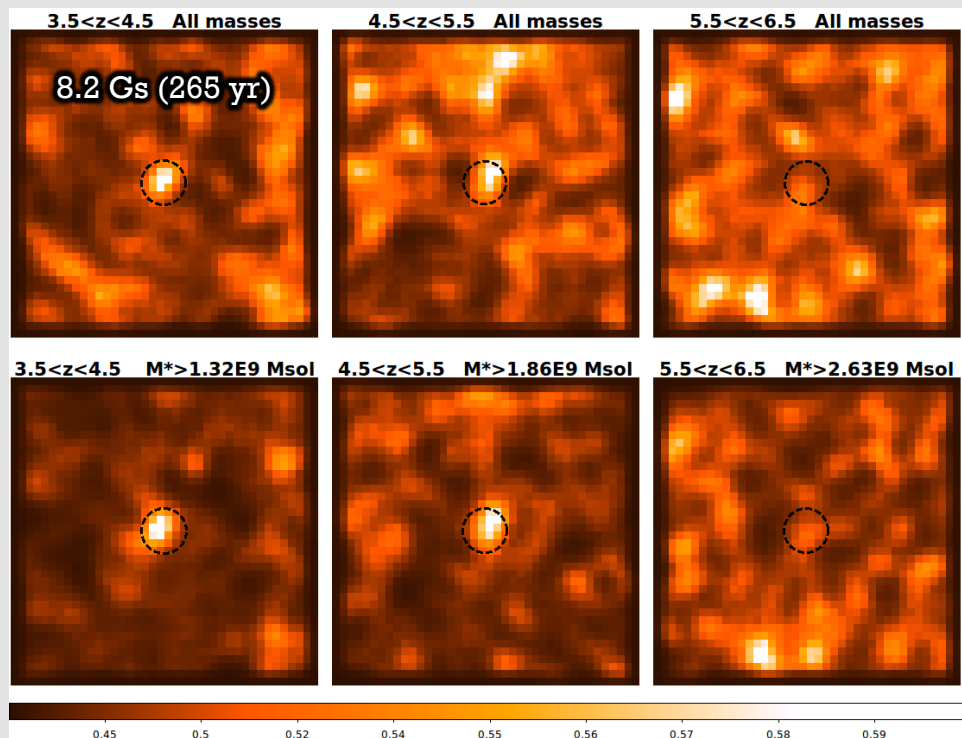
Effective stacked exposure of $(30 \times 1 / 1000 \text{ sec}) = 3 / 100 \text{ sec}$.

7 Ms Chandra Deep Field-South Stacking

Trying to push as faint as possible to constrain SMBH seeds with Chandra.

X-ray stacking of individually undetected galaxies (100-1400 per bin) can provide average X-ray detections to $z = 4.5$ -5.5, and useful upper limits at higher redshifts.

Signal is mostly from massive galaxies, as assessed via sample splitting with 4-fold cross-validation testing.



Reaching Close to X-ray Surveyor Flux Levels - on Average

Table 1. Main properties of the stacked samples.

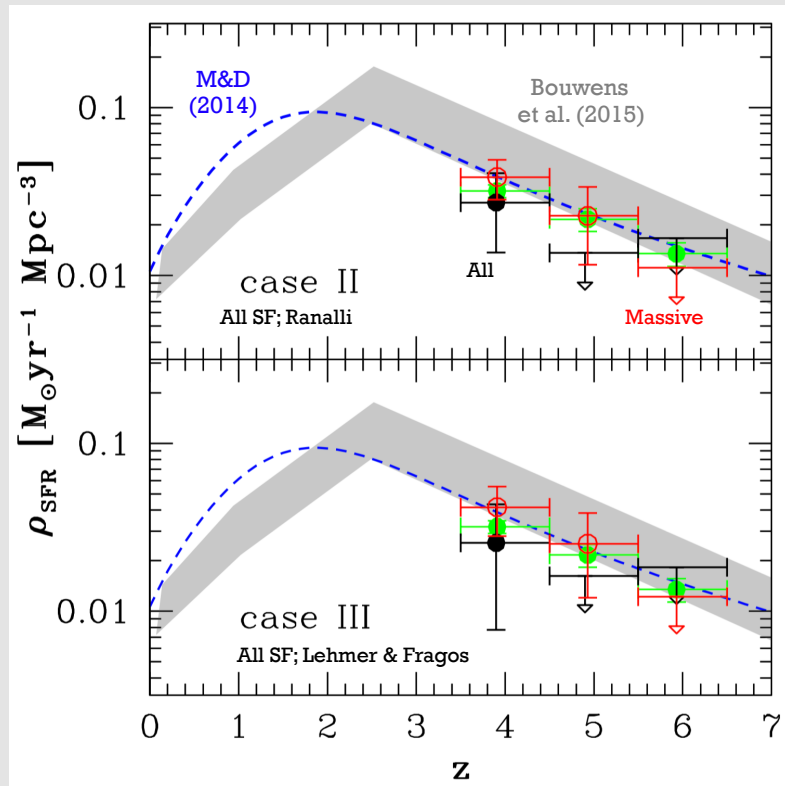
z bin	M_*/M_\odot	N (N^w)	$\langle z^w \rangle$	Exp. 10^9s	$CR^{w,\text{TOT}}$ 10^{-5}cts s^{-1}	$F_{0.5-2\text{keV}}^{w,\text{TOT}}$ $10^{-16}\text{erg cm}^{-2}\text{s}^{-1}$	SNR_{boot} σ	$N_{rand}^{>CR}$	SNR_{rand} σ
(1)	(2)	(3)	(4)	(5)	(6)	(7)	(8)	(9)	(10)
$3.5 \leq z < 4.5$	all	1393 (1441)	3.90	8.16	8.17 ± 4.05	5.11 ± 2.53	2.02	0.0091	2.36
$3.5 \leq z < 4.5$	$\geq 1.32 \times 10^9$	662 (667)	3.91	3.86	11.50 ± 3.08	7.19 ± 1.93	3.74	0.0000*	> 4.00
$4.5 \leq z < 5.5$	all	453 (472)	4.90	2.65	< 2.22	< 1.39	0.87	0.1630	0.98
$4.5 \leq z < 5.5$	$\geq 1.86 \times 10^9$	217 (222)	4.92	1.26	3.66 ± 1.79	2.29 ± 1.12	2.04	0.0034	2.71
$5.5 \leq z < 6.5$	all	230 (241)	5.93	1.35	< 1.61	< 1.01	-0.34	0.6742	-0.45
$5.5 \leq z < 6.5$	$\geq 2.63 \times 10^9$	111 (113)	5.93	0.65	< 1.07	< 0.67	0.25	0.4001	0.25

(1) redshift bin; (2) mass selection: for every redshift bin we first stacked all the galaxies and then the most massive ones, defined as those with M_* larger than the median in that bin; (3) number of CANDELS stacked galaxies and, in parentheses, corresponding weighted number of galaxies (Eq. 1). Note that the stacked number of galaxies in the “massive” samples is close but not equal to half the number of galaxies when no mass cut is applied. The reason is that the mass cut is the median mass of galaxies in the redshift bin, including the galaxies which are not stacked due to their proximity to (or identification with) an X-ray detected source. (4) median weighted redshift (Eq. 2); (5) total exposure time; (6) total (i.e. corrected for the aperture of the extraction radii) weighted net count-rate in the soft band, (7) corresponding total flux, (8) signal-to-noise ratio (SNR) derived from the bootstrap procedure, (9) fraction of runs of the random-position stacking returning a net count rate larger than that found for the sample of real galaxies, based on 10000 runs, and (10) corresponding confidence level. *For this sample we used 50000 runs.

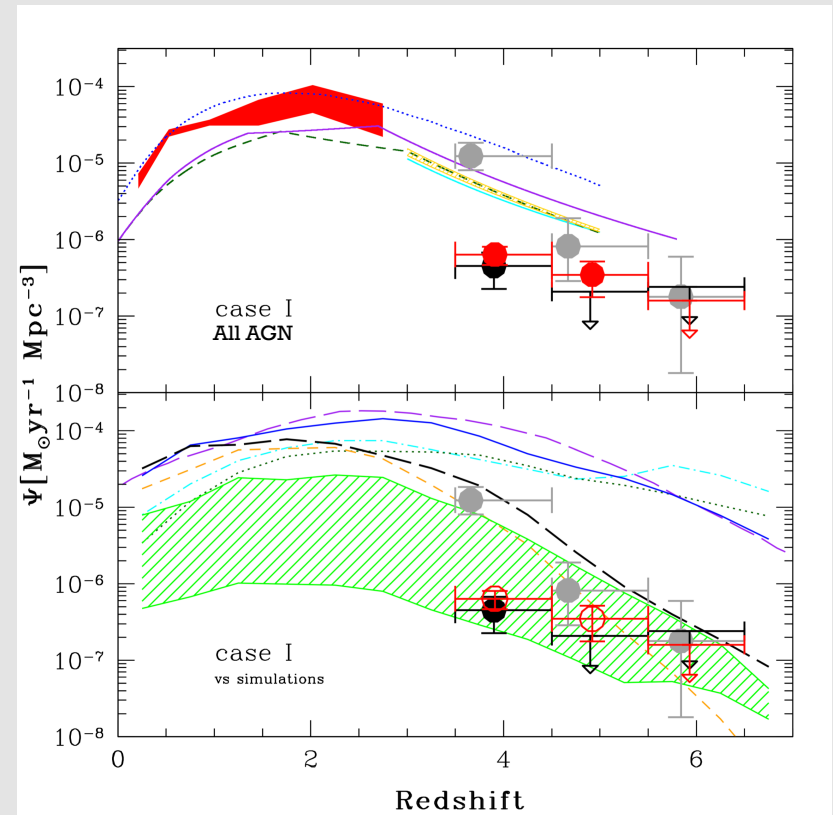
Physical Interpretation of Stacked Flux

Much, and perhaps all, of the observed flux can be attributed to X-ray binaries. Probing HMXBs to $z \sim 5.5$.

Most high-redshift SMBH accretion occurs in short AGN phase – continuous low-rate accretion contribution appears small.



Vito et al. (2016)

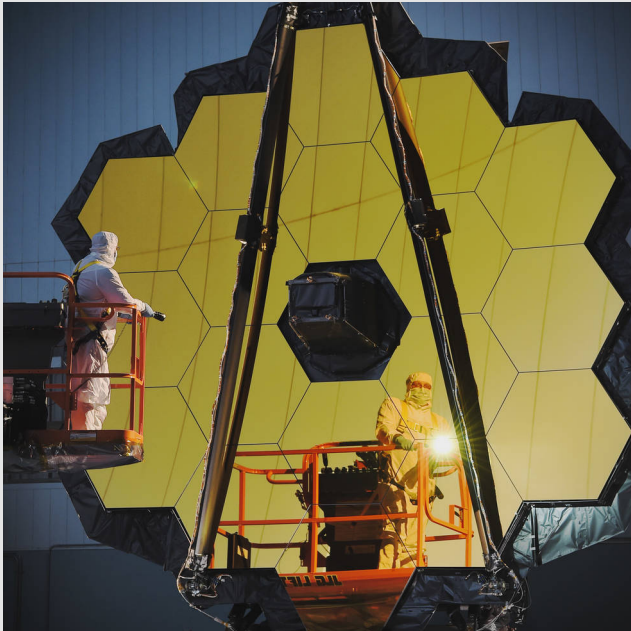


Pushing to the Highest Redshifts with Stacking

Stacking of Lyman Break Galaxy Samples with 7 Ms CDF-S

Vito et al.

z	N	$\langle H \rangle$ mag	Exp. (10^9 s)	CR_{TOT}^w (10^{-5} cts s^{-1})	$F_{0.5-2\text{keV}}^{w,obs,TOT}$ (10^{-16} erg cm^{-2} s^{-1})	SNR_{boot} σ
(1)	(2)	(3)	(4)	(5)	(6)	(7)
~ 4	2444	26.4	14.33	11.30 ± 5.12	7.06 ± 3.20	2.26
~ 5	673	26.7	3.95	< 2.63	< 1.64	0.48
~ 6	259	26.8	1.52	< 1.58	< 0.99	-1.89
~ 7	107	27.1	0.62	< 1.03	< 0.64	0.60
~ 8	36	27.1	0.21	< 0.32	< 0.20	-1.65



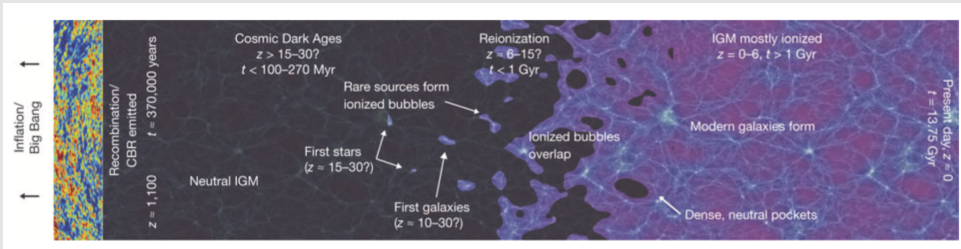
JWST will provide large samples at higher redshifts, better redshift identifications, and better removal of low-redshift interlopers.

Aim to push Chandra stacking analyses to $z \sim 10-15$ with the samples of high-redshift galaxies from JWST in the 7 Ms CDF-S (and other fields).

Also could stack 21-cm selected regions, or perform cross-correlation analyses.

X-ray Surveyor would allow much better stacking.

XRS Connections with 21-cm IGM Probes

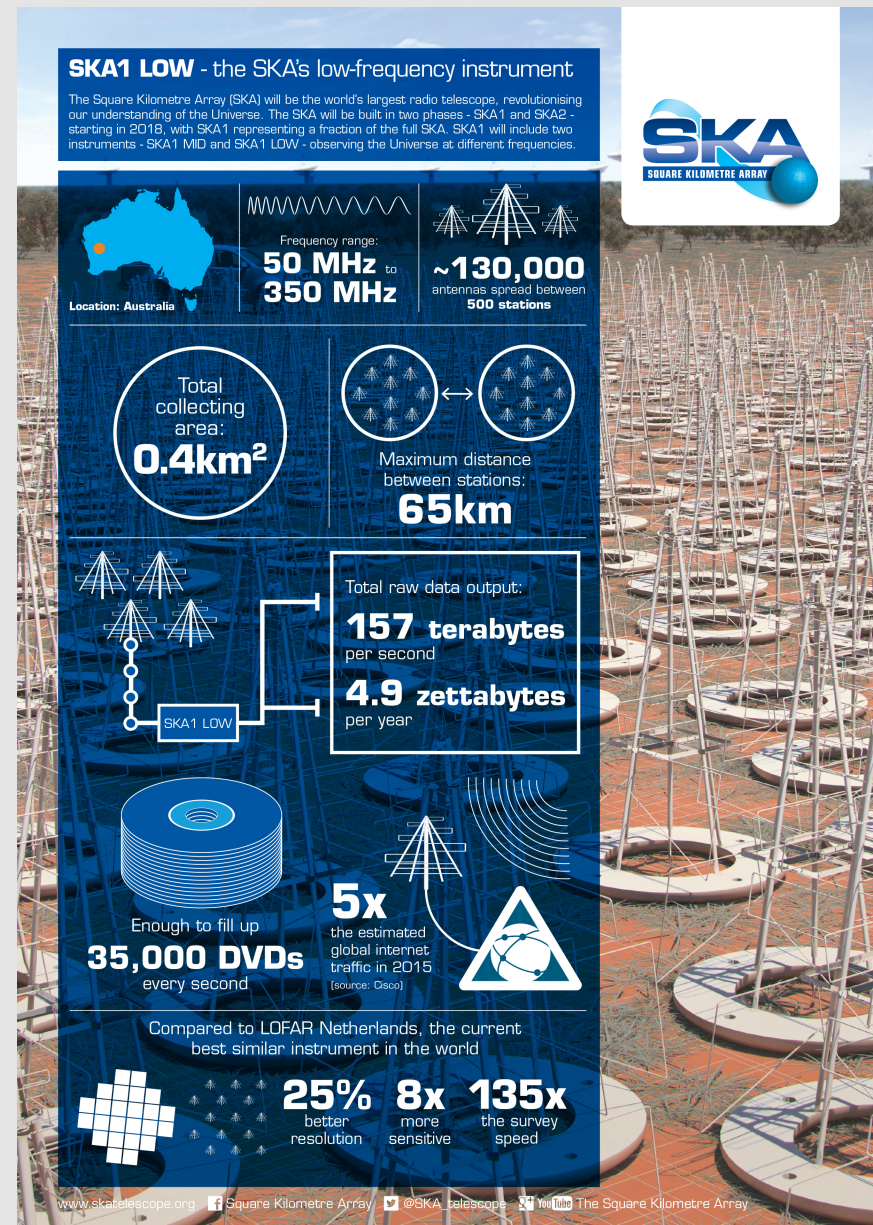


First X-ray sources heated the IGM at $z \sim 10-20$ from $T \sim \text{few K}$ to $T > 10000$ K. They also mildly ionized the IGM (in addition to stars) to the level of ~ 0.001 .

Hydrogen Epoch of Reionization Array (HERA) 2016 March



Many more such experiments ongoing!



Constraining the redshifted 21-cm signal with the unresolved soft X-ray background

Anastasia Fialkov^{1,2*}, Aviad Cohen³, Rennan Barkana^{3,4,5} & Joseph Silk^{5,6,7}

¹ Department of Astronomy, Harvard University, 60 Garden Street, MS – 51, Cambridge, MA, 02138 U.S.A.

² Département de Physique, Ecole Normale Supérieure, CNRS, 24 rue Lhomond, Paris, 75005 France

³ Raymond and Beverly Sackler School of Physics and Astronomy, Tel Aviv University, Tel Aviv 69978, Israel

⁴ Sorbonne Universités, Institut Lagrange de Paris (ILP), Institut d'Astrophysique de Paris, UPMC Univ Paris 06/CNRS

⁵ Department of Astrophysics, University of Oxford, Denys Wilkinson Building, Keble Road, Oxford OX1 3RH, UK

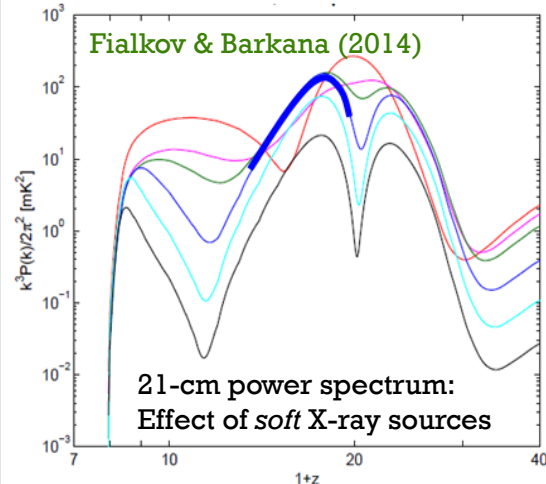
⁶ Sorbonne Universités, UPMC Univ Paris 6 et CNRS, UMR 7095, Institut d'Astrophysique de Paris, 98 bis bd Arago, 75014 Paris, France

⁷ Department of Physics and Astronomy, The Johns Hopkins University, Baltimore, MD 21218, USA

25 February 2016

ABSTRACT

We use the observed unresolved cosmic X-ray background (CXRB) in the soft 0.5 – 2 keV band to constrain the population of high redshift X-ray sources existing before the end of reionization. Because the nature of these sources is poorly understood, we consider hot gas, X-ray binaries and mini-quasars (i.e., sources with soft and hard X-ray spectra) as possible candidates. We show that all types of the considered sources naturally generate a soft band CXRB, but if they actually generate the observed background their efficiency in producing X-rays must be one-to-two orders of magnitude higher than what is normally assumed. We find that the efficiency of hard sources does not have to be increased as strongly as that of the soft ones in order to generate the observed background. In addition, we show that when models are normalized to the CXRB, cosmic heating occurs quite early, and in some cases X-rays become a significant driver of reionization competing with the UV photons, while the expected high-redshift 21-cm signal is reduced. Given the great uncertainty in the efficiency of early X-ray sources, the normalization to the CXRB yields an important upper limit on the effect that high-redshift X-ray sources can have on the thermal history of the Universe and on the 21-cm signal. For completeness, we also consider lower limits on the X-ray heating efficiency arising from recent upper limits on the 21-cm power spectrum. Weak heating would result in a strong 21-cm signal, which would be an easy target for radio telescopes.



Constraining High Redshift X-ray Sources with Next Generation 21 cm Power Spectrum Measurements

Aaron Ewall-Wice^{1 *}, Jacqueline Hewitt¹, Andrei Mesinger², Joshua S. Dillon^{1,3}, Adrian Liu^{4,†}, Jonathan Pober⁵

¹ Dept. of Physics and MIT Kavli Institute, Massachusetts Institute of Technology, Cambridge, MA 02139, USA

² Scuola Normale Superiore, Piazza dei Cavalieri 7, 56126 Pisa, Italy

³ Dept. of Astronomy, UC Berkeley, Berkeley CA 94720

⁴ Berkeley Center for Cosmological Physics, University of California, Berkeley, Berkeley, CA 94720

⁵ Hubble Fellow.

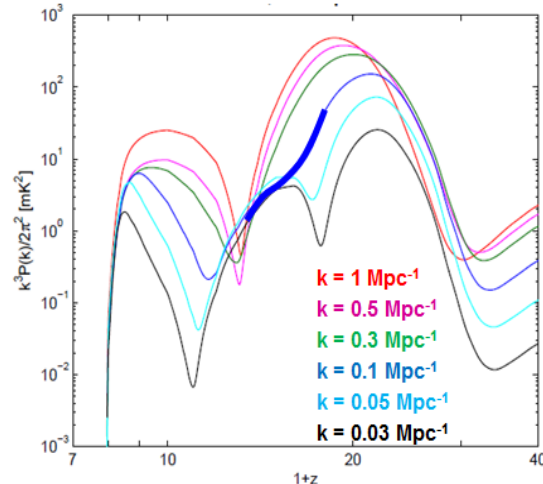
[†] Brown University, Department of Physics, Providence, RI 02912, USA

26 April 2016

ABSTRACT

We use the Fisher matrix formalism and semi-numerical simulations to derive quantitative predictions of the constraints that power spectrum measurements on next-generation interferometers, such as the Hydrogen Epoch of Reionization Array (HERA) and the Square Kilometre Array (SKA), will place on the characteristics of the X-ray sources that heated the high redshift intergalactic medium. Incorporating observations between $z = 5$ and $z = 25$, we find that the proposed 331 element HERA and SKA phase 1 will be capable of placing $\lesssim 10\%$ constraints on the spectral properties of these first X-ray sources, even if one is unable to perform measurements within the foreground contaminated “wedge” or the FM band. When accounting for the enhancement in power spectrum amplitude from spin temperature fluctuations, we find that the observable signatures of reionization extend well beyond the peak in the power spectrum usually associated with it. We also find that lower redshift degeneracies between the signatures of heating and reionization physics lead to errors on reionization parameters that are significantly greater than previously predicted. Observations over the heating epoch are able to break these degeneracies and improve our constraints considerably. For these two reasons, 21 cm observations during the heating epoch significantly enhance our understanding of reionization as well.

Key words: dark ages, reionization, first stars – techniques: interferometric – radio lines: general – X-rays: galaxies

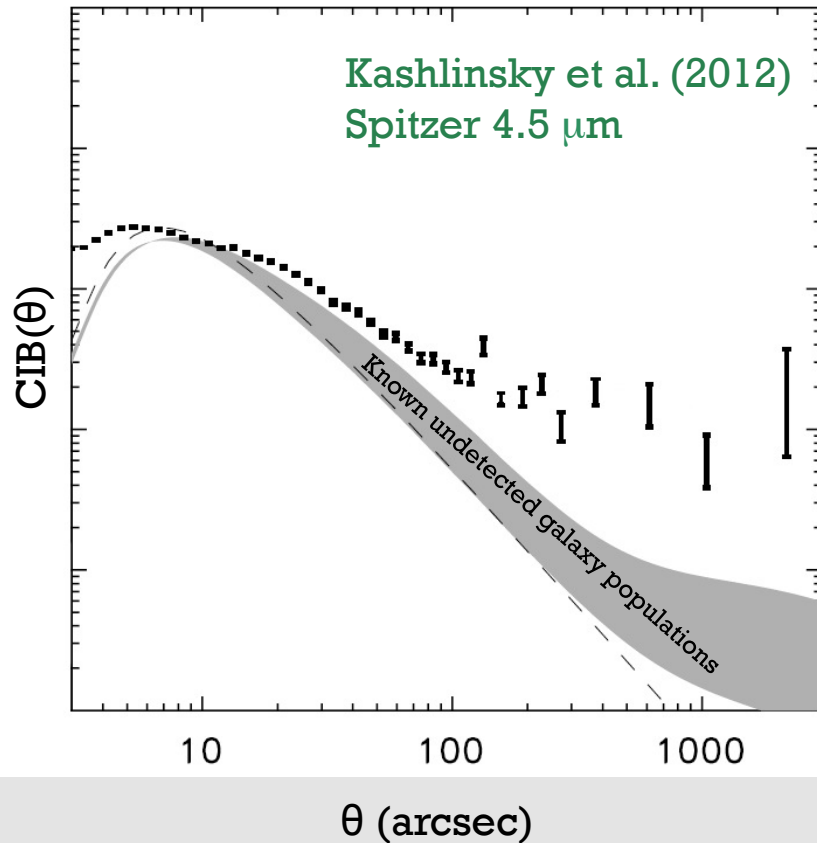


Effect of *hard* X-ray sources (longer path length - no heating fluctuations on scales smaller than mean-free-path)

XRS can probe these X-ray sources directly, and can combine with 21-cm IGM constraints. Also perform, e.g., cross-correlation analyses.

X-ray vs. NIR Background Correlations

CIB Fluctuation Power Spectrum Shows an Unexplained Excess on Large Scales wrt. Known Galaxy Populations



CROSS-CORRELATING COSMIC INFRARED AND X-RAY BACKGROUND FLUCTUATIONS: EVIDENCE OF SIGNIFICANT BLACK HOLE POPULATIONS AMONG THE CIB SOURCES

N. CAPPELLUTI^{1,2}, A. KASHLINSKY^{3,4}, R. G. ARENDT^{2,3}, A. COMASTRI¹, G. G. FAZIO⁵, A. FINOGUENOV^{2,6}, G. HASINGER⁷, J. C. MATHER^{3,8}, T. MIYAJI⁹, AND S. H. MOSELEY^{3,8}

¹ INAF-Osservatorio Astronomico di Bologna, Via Ranzani 1, I-40127 Bologna, Italy

² University of Maryland, Baltimore County, 1000 Hilltop Circle, Baltimore, MD 21250, USA

³ Observational Cosmology Laboratory, Code 665, Goddard Space Flight Center, Greenbelt MD 20771, USA

⁴ SSAI, 10210 Greenbelt Road, Suite 600, Lanham, MD 20706, USA

⁵ Harvard Smithsonian Center for Astrophysics, 60 Garden Street, Cambridge, MA 02138, USA

⁶ Department of Physics, University of Helsinki, Gustaf Hållströmin katu 2a, FI-00014 Helsinki, Finland

⁷ Institute for Astronomy, University of Hawaii, 2680 Woodlawn Drive, Honolulu, HI 96822, USA

⁸ NASA, Greenbelt, MD 20771, USA

⁹ Instituto de Astronomía, Universidad Nacional Autónoma de México, Km 103 Carret. Tijuana-Ensenada,

Ensenada 22860, BC, Mexico

Received 2012 October 18; accepted 2013 April 7; published 2013 May 6

ABSTRACT

In order to understand the nature of the sources producing the recently uncovered cosmic infrared background (CIB) fluctuations, we study cross-correlations between the fluctuations in the source-subtracted CIB from *Spitzer*/IRAC data and the unresolved cosmic X-ray background from deep *Chandra* observations. Our study uses data from the EGS/AEGIS field, where both data sets cover an $\approx 8' \times 45'$ region of the sky. Our measurement is the cross-power spectrum between the IR and X-ray data. The cross-power signal between the IRAC maps at $3.6 \mu\text{m}$ and $4.5 \mu\text{m}$ and the *Chandra* $[0.5-2]$ keV data has been detected, at angular scales $\gtrsim 20''$, with an overall significance of $\approx 3.8\sigma$ and $\approx 5.6\sigma$, respectively. At the same time we find no evidence of significant cross-correlations at the harder *Chandra* bands. The cross-correlation signal is produced by individual IR sources with $3.6 \mu\text{m}$ and $4.5 \mu\text{m}$ magnitudes $m_{\text{AB}} \gtrsim 25-26$ and $[0.5-2]$ keV X-ray fluxes $\ll 7 \times 10^{-17} \text{ erg cm}^2 \text{ s}^{-1}$. We determine that at least 15%–25% of the large scale power of the CIB fluctuations is correlated with the spatial power spectrum of the X-ray fluctuations. If this correlation is attributed to emission from accretion processes at both IR and X-ray wavelengths, this implies a much higher fraction of accreting black holes than among the known populations. We discuss the various possible origins for the cross-power signal and show that neither local foregrounds nor the known remaining normal galaxies and active galactic nuclei can reproduce the measurements. These observational results are an important new constraint on theoretical modeling of the near-IR CIB fluctuations.

CROSS-CORRELATION BETWEEN X-RAY AND OPTICAL/NEAR-INFRARED BACKGROUND INTENSITY FLUCTUATIONS

KETRON MITCHELL-WYNN¹, ASANTHA COORAY¹, YONGQUAN XUE², BIN LUO^{3,4}, WILLIAM BRANDT^{5,6,7}, ANTON KOEKEMOER⁸

¹ Department of Physics & Astronomy, University of California, Irvine, CA 92697

² CAS Key Laboratory for Researches in Galaxies and Cosmology, Center for Astrophysics, Department of Astronomy, University of Science and Technology of China, Chinese Academy of Sciences, Hefei, Anhui 230026, China

³ School of Astronomy and Space Science, Nanjing University, Nanjing, 210093, China

⁴ Key Laboratory of Modern Astronomy and Astrophysics (Nanjing University), Ministry of Education, Nanjing 210093, China

⁵ Department of Astronomy & Astrophysics, Pennsylvania State University, University Park, PA, 16802

⁶ Institute for Gravitation and the Cosmos, Pennsylvania State University, 525 Davey Lab, University Park, PA 16802

⁷ Department of Physics, 104 Davey Lab, The Pennsylvania State University, University Park, PA 16802, USA and

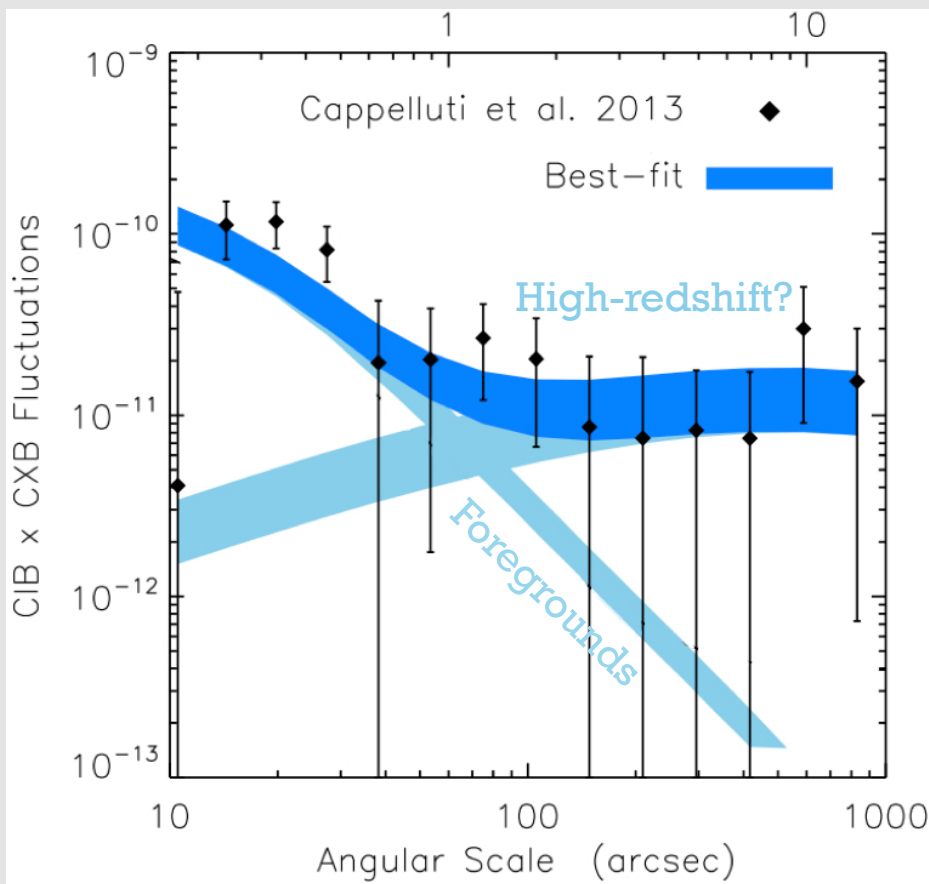
⁸ Space Telescope Science Institute, 3700 San Martin Drive, Baltimore, MD 21218, USA

Draft version October 7, 2016

ABSTRACT

Angular power spectra of optical and infrared background anisotropies at wavelengths between 0.5 to $5 \mu\text{m}$ are a useful probe of faint sources present during reionization, in addition to faint galaxies and diffuse signals at low redshift. The cross-correlation of these fluctuations with backgrounds at other wavelengths can be used to separate some of these signals. A previous study on the cross-correlation between X-ray and *Spitzer* fluctuations at $3.6 \mu\text{m}$ and $4.5 \mu\text{m}$ has been interpreted as evidence for direct collapse blackholes (DCBHs) present at $z > 12$. Here we return to this cross-correlation and study its wavelength dependence from 0.5 to $4.5 \mu\text{m}$ using *Hubble* and *Spitzer* data in combination with a subset of the 4 Ms *Chandra* observations in GOODS-S/ECDFS. Our study involves five *Hubble* bands at 0.6, 0.7, 0.85, 1.25 and $1.6 \mu\text{m}$, and two *Spitzer*-IRAC bands at $3.6 \mu\text{m}$ and $4.5 \mu\text{m}$. We confirm the previously seen cross-correlation between $3.6 \mu\text{m}$ ($4.5 \mu\text{m}$) and X-rays with 3.7σ (4.2σ) and 2.7σ (3.7σ) detections in the soft $[0.5-2]$ keV and hard $[2-8]$ keV X-ray bands, respectively, at angular scales above 20 arcseconds. The cross-correlation of X-rays with *Hubble* is largely anticorrelated, ranging between the levels of $1.4-3.5\sigma$ for all the *Hubble* and X-ray bands. This lack of correlation in the shorter optical/NIR bands implies the sources responsible for the cosmic infrared background at 3.6 and $4.5 \mu\text{m}$ are at least partly dissimilar to those at $1.6 \mu\text{m}$ and shorter.

X-ray vs. NIR Background Correlations



Coherent CIB x CXB fluctuations found.

The large-scale power is consistent with a population of direct-collapse black holes at $z > 10$ (e.g., Yue et al. 2013).

But interpretation is controversial. Also might be from intra-halo light at $z \sim 1-4$.

Background and small FOV of Chandra are limiting factors for current analyses.

X-ray Surveyor and next-generation infrared/optical surveyors can perform much better CIB x CXB measurements.

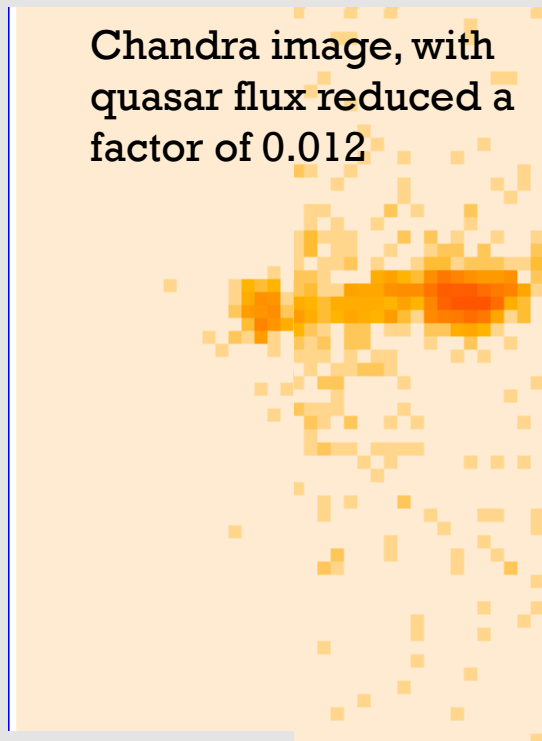
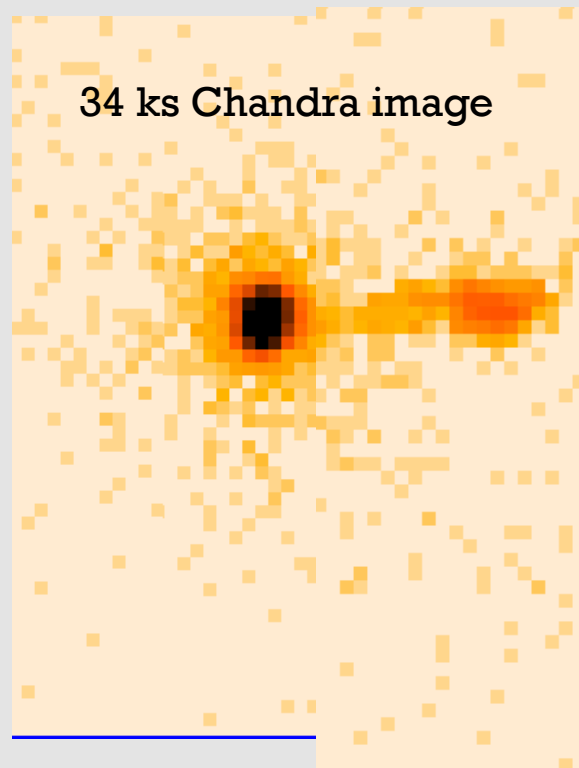
Aim to measure typical seed masses, total mass in seeds, and redshift of formation.

Additional Science

Inverse-Compton X-ray Jets Maintain Their Surface Brightness (Almost) Independent of Redshift

The inverse-Compton scattered X-rays are proportional to the CMB energy density. The increase of that density proportional to $(1+z)^4$ cancels the cosmological diminution of surface brightness by the factor $(1+z)^{-4}$

Example: PKS 0637-752 is a quasar at $z = 0.657$ (left). Right panel shows appearance at $z = 4$. X-ray Surveyor should obtain similar images in 1 ks.

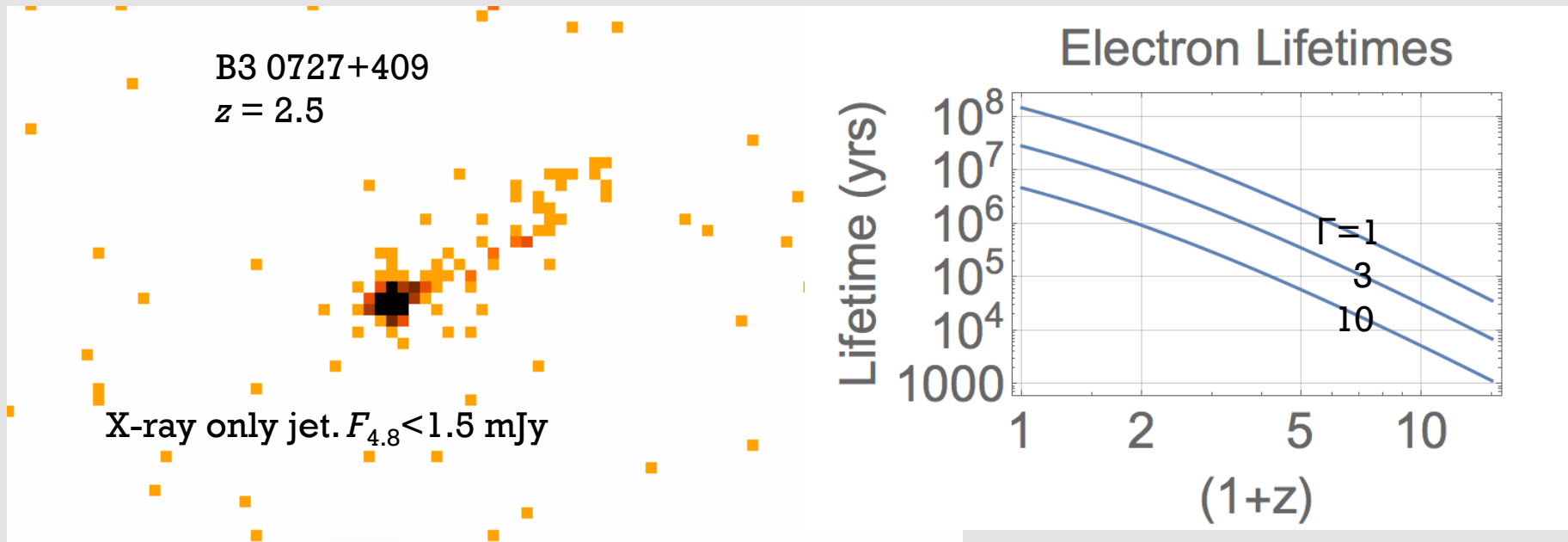


e.g., Rees & Setti (1968);
Schwartz (2002)

Inverse-Compton X-ray Jets

At large redshifts, the quasar will be much fainter and may not be seen, and the radio emission is also much fainter and may not be seen.

In addition, the lifetime of GHz emitting electrons is ~ 100 times shorter than that of the X-ray emitting electrons, for which the lifetimes are shown below.



Simionescu et al. (2016)

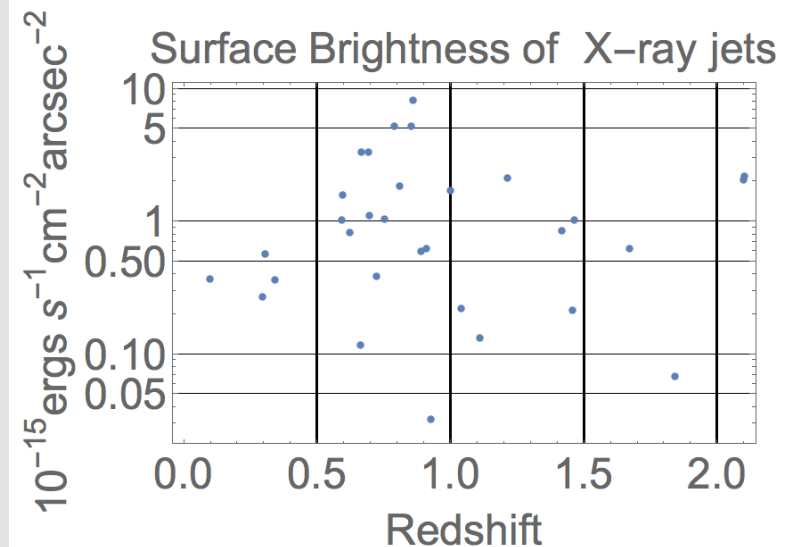
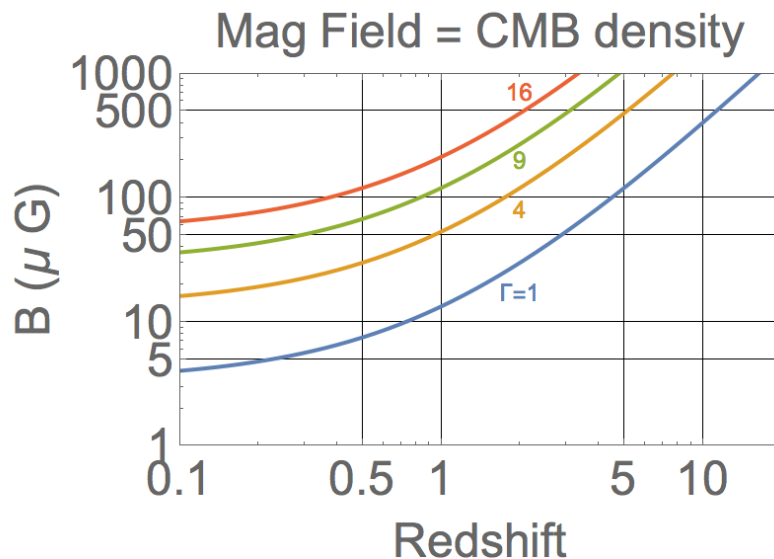
Inverse Compton X-ray Jets

At large redshift, relativistic jets must emit inverse Compton keV X-rays, unless the magnetic field strength is larger than plotted (left) for the given bulk Lorentz factor of the jet.

Chandra measures surface brightnesses around $10^{-15} \text{ erg cm}^{-2} \text{ s}^{-1} \text{ arcsec}^{-2}$ (right), XRS background is expected to be around $1.7 \times 10^{-19} \text{ erg cm}^{-2} \text{ s}^{-1} \text{ arcsec}^{-2}$.

Observing strategy: Layered surveys
Unidentified X-ray sources from all sky surveys
Large redshift radio and optical AGN

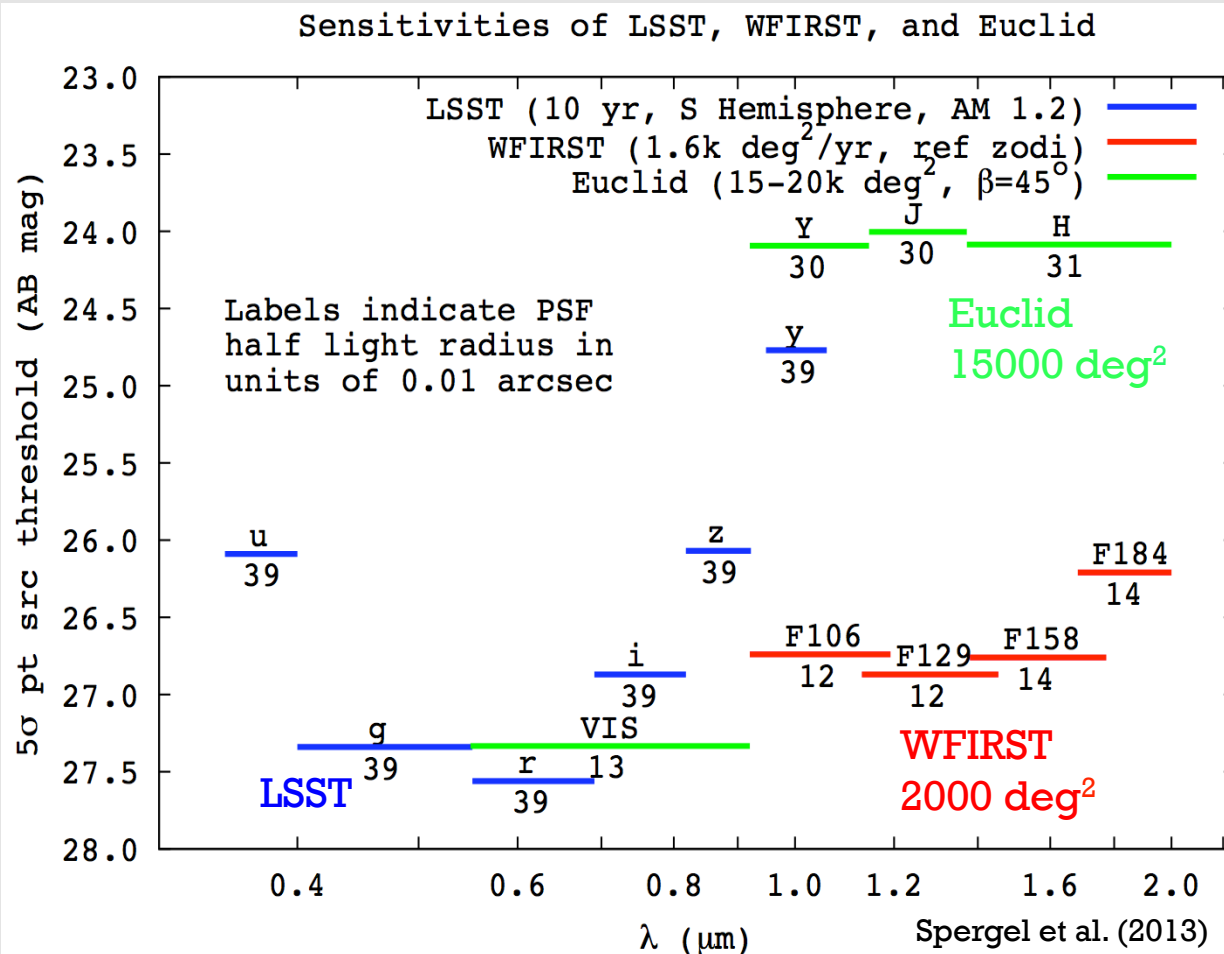
Marshall et al. (2005, 2011)



The End

Extra Slides

High-Redshift Quasars from Euclid, WFIRST, and LSST



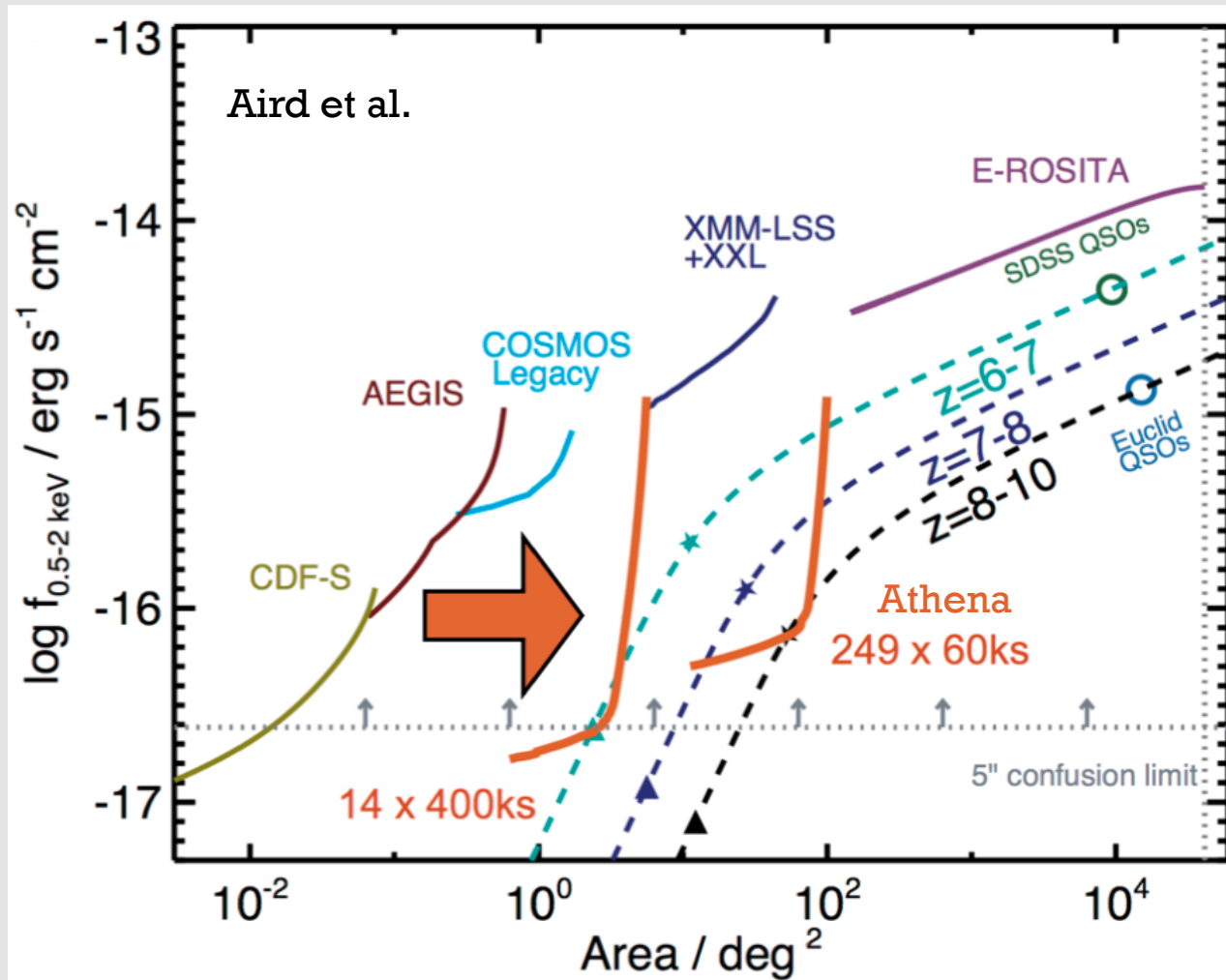
Combination of Euclid, WFIRST, and LSST will be very powerful for finding the first quasars.

Euclid should deliver ~ 1400 luminous quasars at $z > 7$.

WFIRST+LSST will push considerably deeper than Euclid over $\sim 15\%$ of the area.

Expect ~ 1500 quasars at $z > 7$ (~ 30 at $z > 10$).

Athena Can Generate a Lot More of What We Currently Have Only in Small Amounts

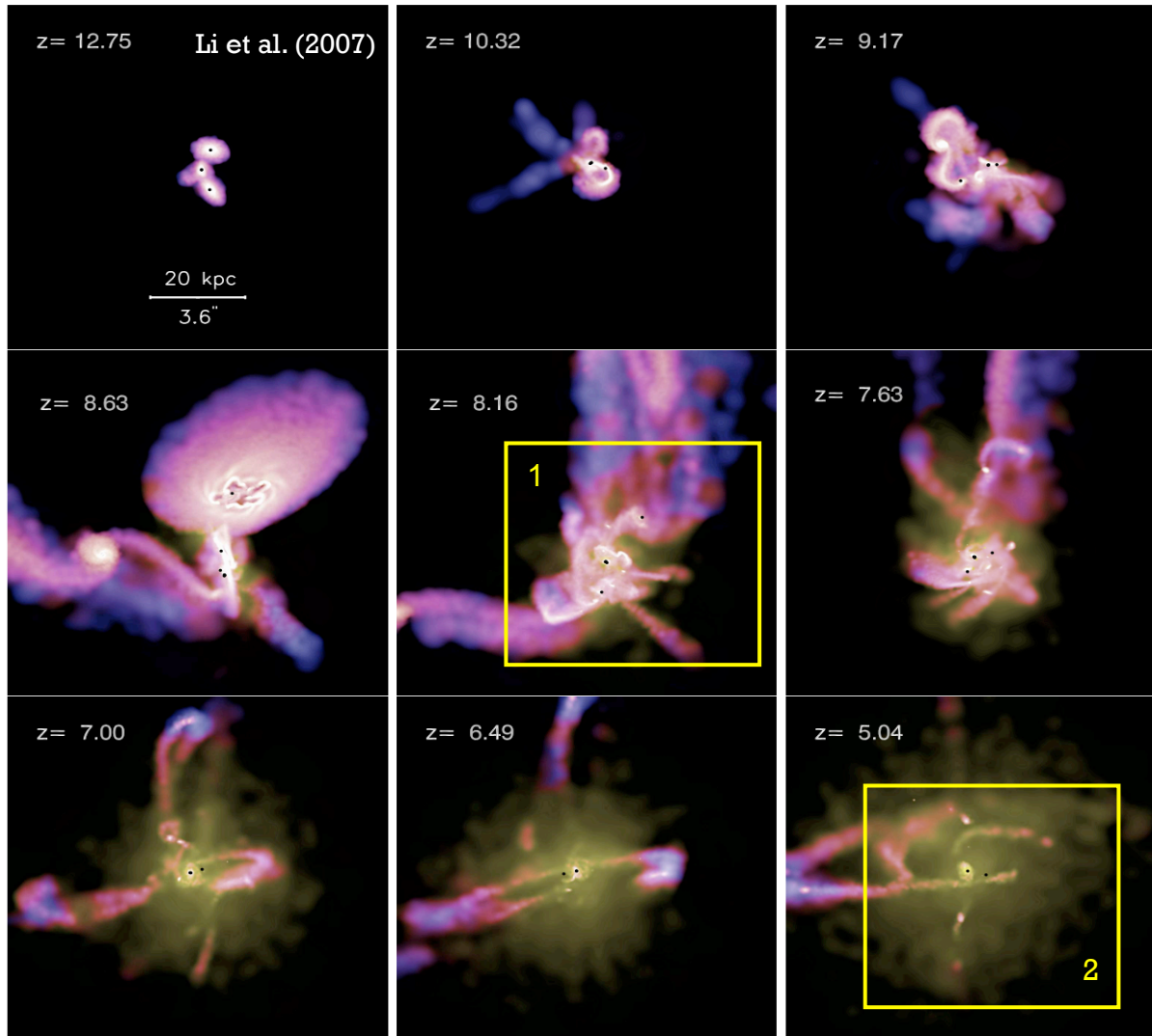


A very good thing for getting reliable AGN source statistics at $z \sim 5-10$.

Will provide a lot more photons for source spectral and variability diagnostics.

Source confusion with a 5" PSF will prevent it from going deeper than the deepest Chandra observations.

Simulation of the Formation of a $z \sim 6$ Quasar from Hierarchical Galaxy Mergers

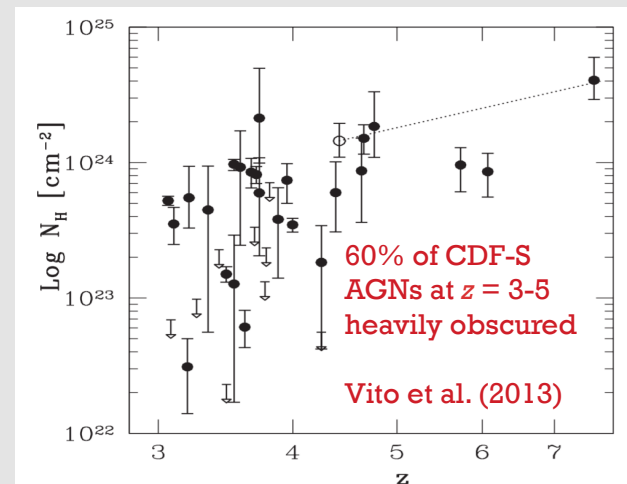
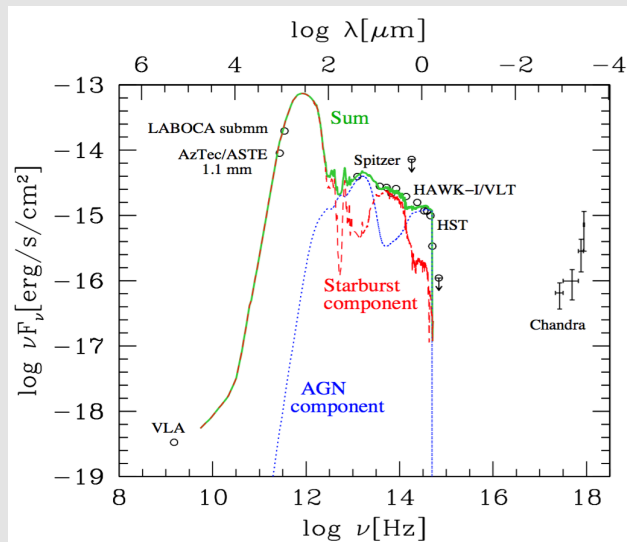
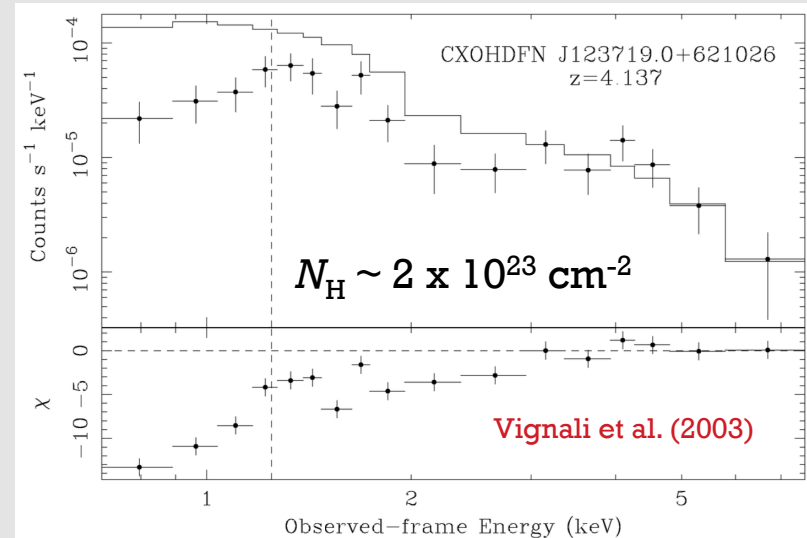
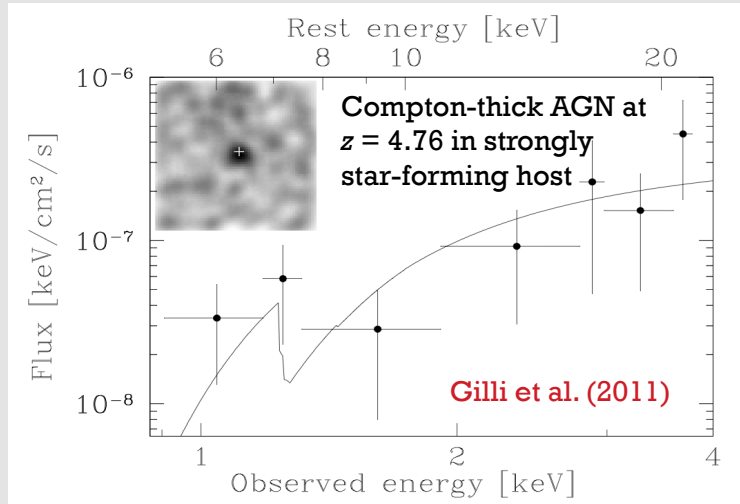


Gas density and temperature
for high-redshift quasar host

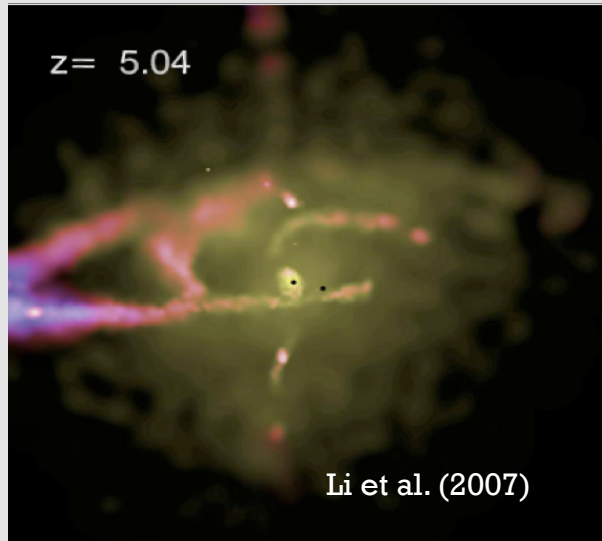
Albeit at somewhat lower
redshifts, we observe similar
phenomena at $z \sim 4-5$:

- (1) X-ray obscured protoquasars
of moderate luminosity
- (2) powerful winds from
luminous quasars, likely
capable of host feedback

X-ray Obscured Protoquasars of Moderate Luminosity at $z \sim 4-5$



Powerful Winds from Luminous High-Redshift Quasars

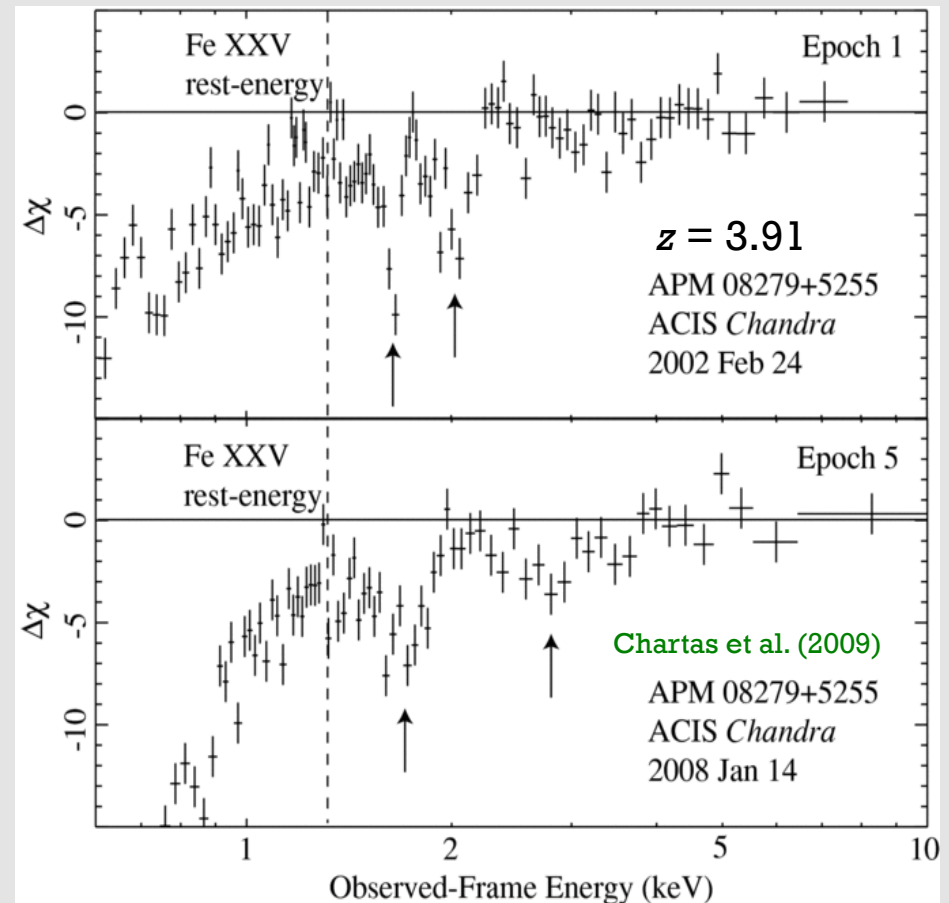


Implied X-ray velocity is $v \sim 0.2-0.4c$.

Implied mass-outflow rate is $\sim 10-30 M_{\odot} \text{ yr}^{-1}$
and kinetic luminosity is $\sim 10^{46-47} \text{ erg s}^{-1}$.

Could be present but undetected in many other high-redshift quasars (had boost from gravitational lensing).

X-ray Broad Absorption Lines from Iron K Indicating a Powerful Wind – High-Redshift Feedback in Action?

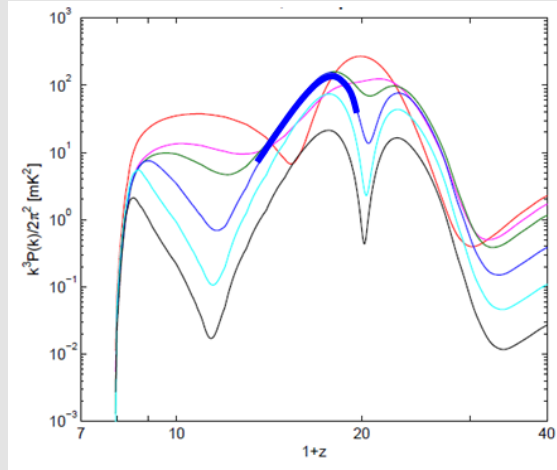


Nature of First X-ray Sources

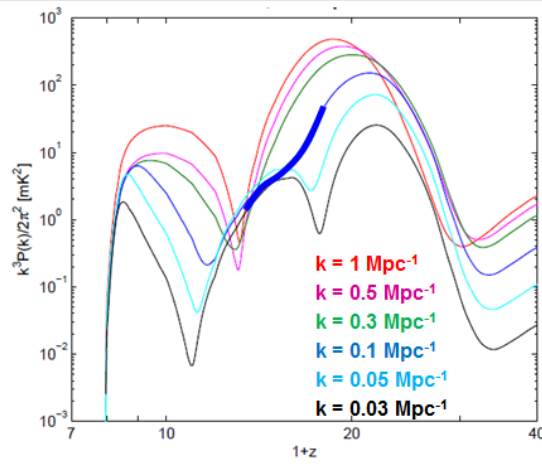
First X-ray sources heated the Inter-Galactic Medium (IGM) at redshifts $z \sim 10-20$ from $T \sim \text{few Kelvin}$ to $T > 10000 \text{ Kelvin}$. They also mildly ionized the IGM (in addition to stars) to the level of ~ 0.001 .

Their nature is unknown and candidates discussed in literature are: high mass X-ray binaries, AGN, hot ISM, shocks, dark matter annihilation.

The nature of these sources can either be probed directly or via their impact on IGM seen in the 21-cm line.

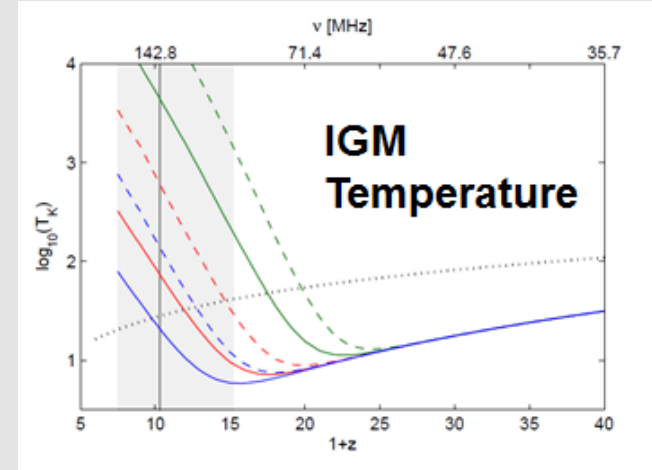


21-cm power spectrum,
effect of **soft** X-ray sources



21-cm power spectrum,
effect of **hard** X-ray sources

Fialkov & Barkana (2014)
Fialkov & Loeb (2016)



Temperature of neutral IGM,
hard sources (solid), **soft** (das),
normal X-ray efficiency (red),
weak (blue), strong (green)

Using XRS to Identify X-ray Sources at High Redshifts

XRS should be sensitive enough to probe brightest star forming regions at the Dawn of star formation.

If X-ray binaries are the dominant X-ray heating source before the end of Reionization ($z > 6$), the brightest

star forming regions at $z = 9$ would emit observable flux of

$S = 1.2 \times 10^{-13}$ erg/s/cm²/keV per deg² (at observable 1 keV), while star forming regions at $z = 13$ are expected to yield $S = 8 \times 10^{-14}$ erg/s/cm²/keV per deg². This flux should be well within reach of X-ray surveyor.

Statistics of such sources will help to probe star formation scenarios at high redshifts.

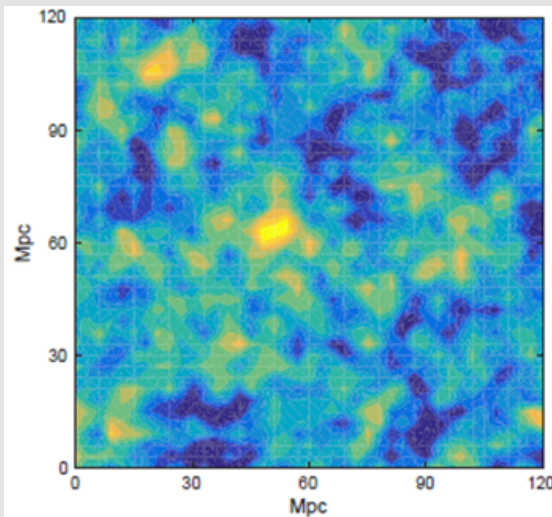


Illustration: Bright X-ray regions at Cosmic Dawn

Fialkov et al. in prep.

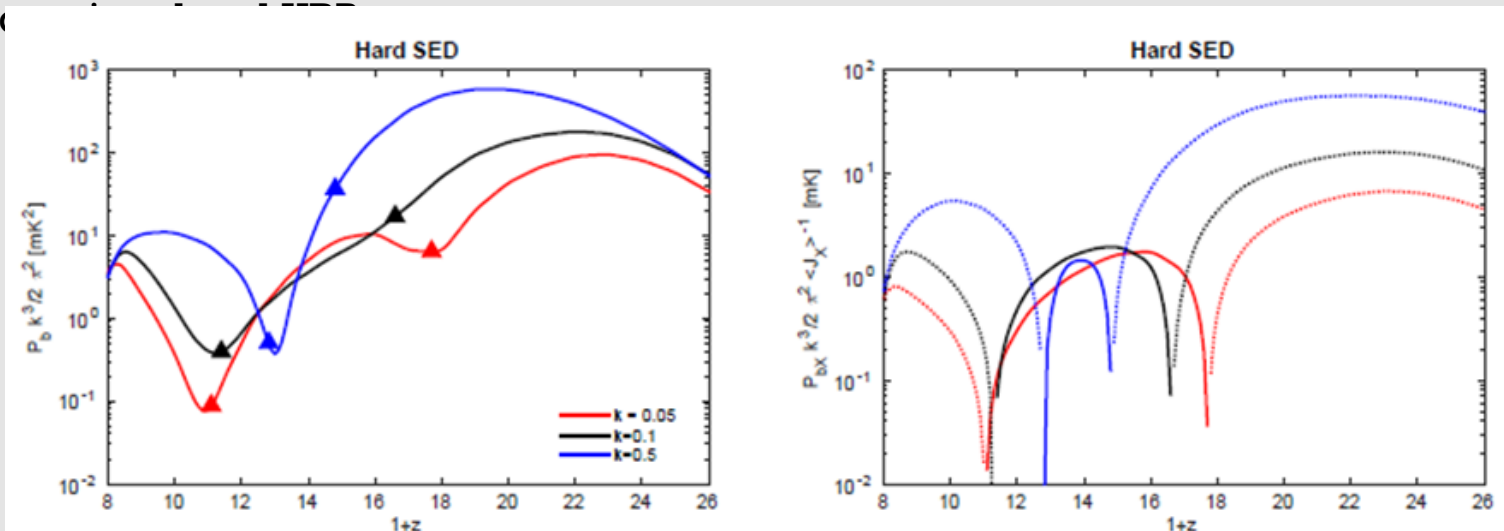
Large-scale Fluctuations of X-ray Background

Fluctuations in the cosmological X-ray background could offer a unique way to constrain the nature of high- z ($z > 6$) X-ray sources and their effect on large scales.

Synergy with radio: cross-correlation with the 21-cm signal observed by the future Square Kilometer Array (if fluctuations in the cosmological background are observed).

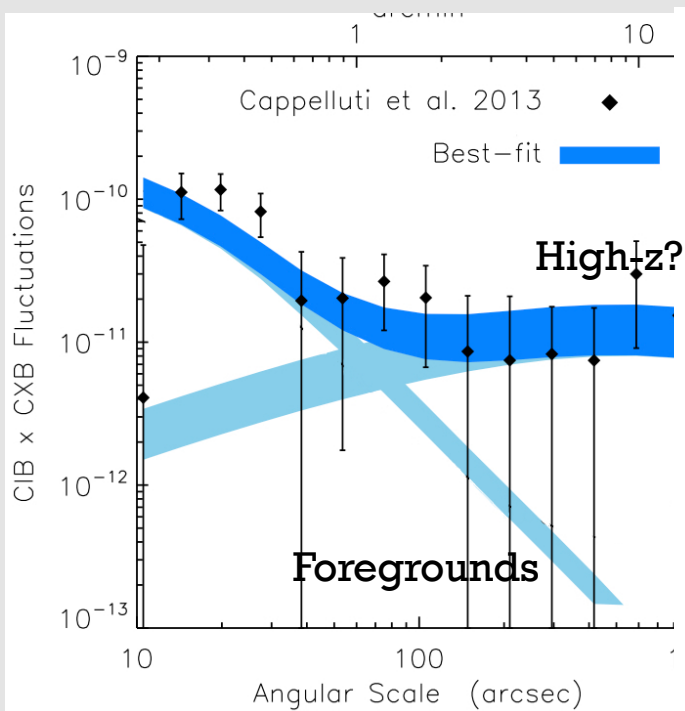
Science: Will allow to probe the epoch in global cosmic history of the Universe over which X-rays had a role (global heating of the IGM)

Left: 21-cm power spectrum vs redshift. Right: cross-correlation between the 21-cm

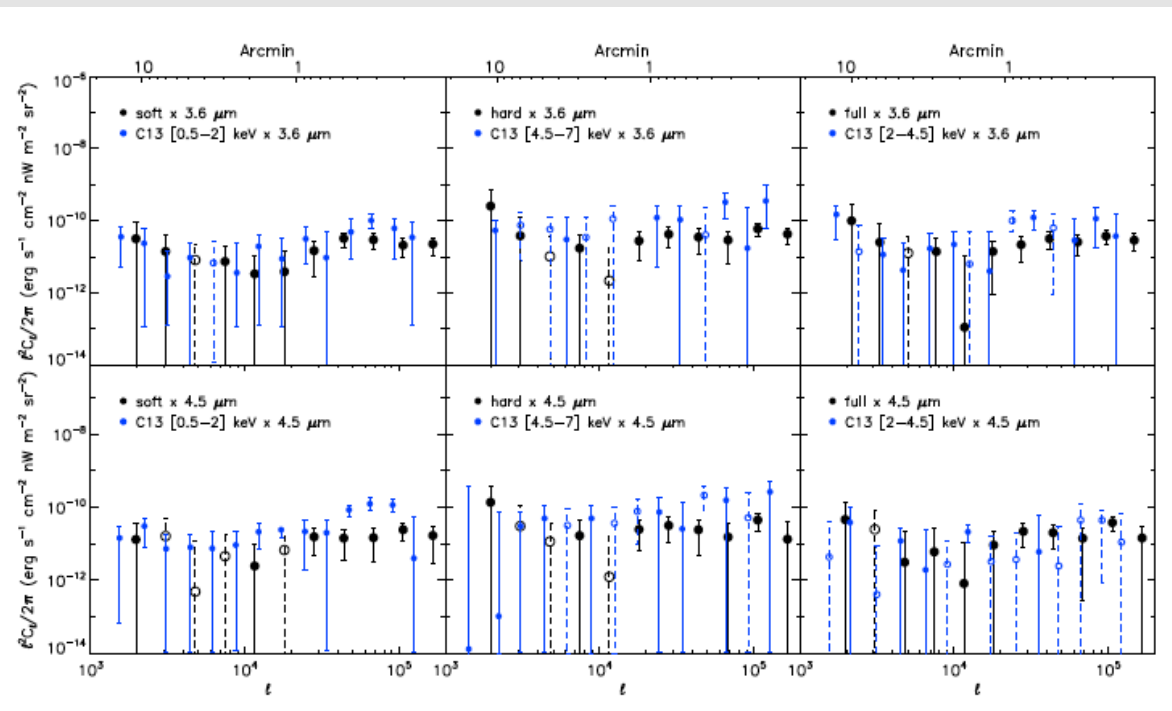


Fialkov et al. in prep

Surprising coherent fluctuations with CXB



CAPPELLUTI+13



MITCHELL-WYNNE+16

THE LARGE SCALE POWER IS CONSISTENT WITH A POPULATION OF DCBH AT $Z > 10$ BUT LARGE SCALE CROSS-POWER IS STILL WEAK

WITH XRS WE WILL STUDY THE LARGE SCALES AND THANK TO THE LARGE SURVEY AREA AND PHOTON STATISTICS WE WILL BE ABLE TO FIT HIGH-Z BH POPULATIONS SYNTHESIS MODELS

DCBH on joint CIB-CXB fluctuations

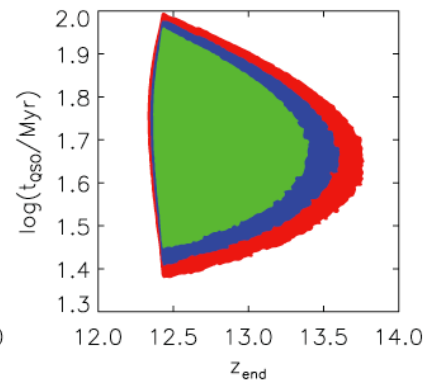
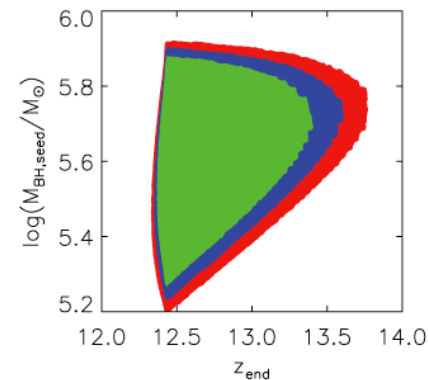
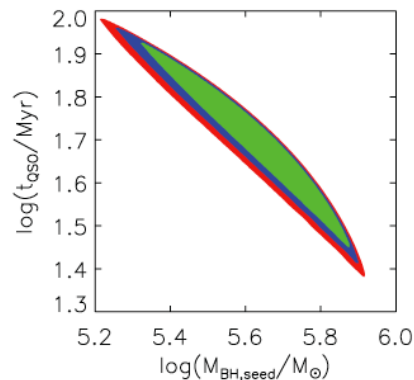
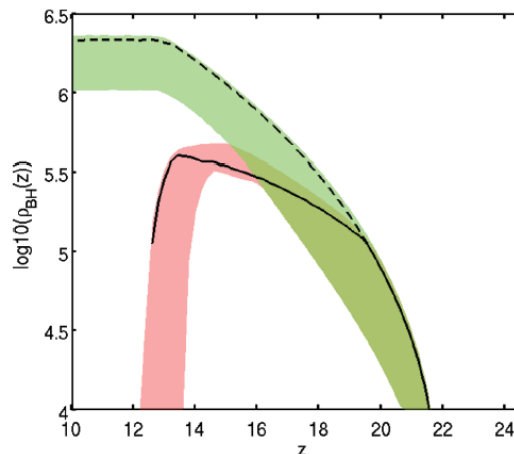
Joint CIB vs CXB fluctuations can be explained with DCBHs.

The poor statistics at large scales does not allow to fit model. So far DCBH growth only would saturate the accreted mass density by $z \sim 12$. Better measurements at large scales are a must.

Science: Will “measure” the total mass in DCBH, and the typical mass of DCBH seeds, and redshift of formation

The Accreted mass density of DCBH necessary explain the joint fluctuations very rapidly saturates

DCBH fit result to cross-power spectra.



This is the Title

Some text.